Radiation Synthesis and Characterization of Poly(Vinyl Alcohol)/ Acrylamide/ TiO2/ SiO2 Nanocomposite for Removal of Metal Ion and Dye From Waste Water

Ahmed Elbarbary (amelbarbary@yahoo.com)

Radiation Research of Polymer Chemistry Department, National Center for Radiation Research and Technology, Egyptian Atomic Energy Authority, Cairo, Egypt https://orcid.org/0000-0001-5318-602X

Yasser H. Gad

Radiation Research of Polymer Chemistry Department, National Center for Radiation Research and Technology, Egyptian Atomic Energy Authority, Cairo, Egypt

Research Article

Keywords: radiation polymerization, poly(vinyl alcohol), acrylamide, TiO2, SiO2, nanocomposite, basic blue 3 dye, copper ions. adsorption, removal

Posted Date: March 24th, 2021

DOI: https://doi.org/10.21203/rs.3.rs-346264/v1

Radiation synthesis and characterization of poly(vinyl alcohol)/ acrylamide/ TiO_2/ SiO_2 nanocomposite for removal of metal ion and dye from waste water

Ahmed M. Elbarbary* and Yasser H. Gad
Radiation Research of Polymer Chemistry Department, National Center for Radiation Research and Technology, Egyptian Atomic Energy Authority, Cairo, Egypt

Abstract

An effective and novel adsorbent of poly(vinyl alcohol)/polyacrylamide/TiO_2/SiO_2 (PVA-co-AAm/TiO_2/SiO_2) nanocomposite synthesized by γ-irradiation polymerization of PVA and AAm in presence of TiO_2/SiO_2 nanoparticles at different irradiation doses (10, 30 and 50 kGy) for removal of Cu(II) ions and basic blue 3 dye from their aqueous solutions. FT-IR, TEM, XRD, SEM, EDS and DLS analyzed the chemical properties of nanocomposites. The nanocomposite prepared at 30 kGy (PVA-co-AAm/TiO_2/SiO_2-30) shows high swelling of 197.7 (%) and gelation of 93.1 %. The adsorption capacity (mg/g) and removal (%) of basic blue 3 dye and Cu(II) ions onto nanocomposites by varying experimental conditions were investigated. The PVA-co-AAm/TiO_2/SiO_2-30 showed high adsorption capacity 3 folds rather than PVA-co-AAm. The equilibrium adsorption for basic blue 3 dye and Cu(II) was 123.9 mg/g and 190.3 mg/g with removal of 82.6 and 95.1 %, respectively. The results of the adsorption of dye or metal ions follow the Pseudo-second order adsorption kinetic, fit with the Langmuir isotherm and the adsorption process is endothermic and spontaneous in nature. The results revealed that the PVA-co-AAm/TiO_2/SiO_2 nanocomposites could be employed as an effectual adsorbent for adsorption of basic blue dye and Cu(II) ions from wastewater with high adsorption capacity and recovery.

Keywords: radiation polymerization; poly(vinyl alcohol), acrylamide; TiO_2; SiO_2, nanocomposite; basic blue 3 dye; copper ions; adsorption; removal

Corresponding author: Ahmed M. Elbarbary
E.mail:amelbarbary@yahoo.com, ahmed.elbarbary@eaea.org.eg

1. Introduction

Industrial wastewater are regularly contaminated with an assortment of compounds that give a negative effects on the environment.[1] A great amount of heavy metals for example Cu (II) ions released in wastewater by industries wastes.[2] One of the difficulties correlated with the occurrence of heavy metals in wastewater is that they are not biodegradable in an aquatic media, and so they can be consumed by organisms, and consequently, go into the food chain. Human body contains copper, and it plays a significant function for the development of bones and tissues or in enzyme creation.[3] On the other hand, an overload of Cu (II) ions and its deposition in the body is poisonous and causes a severe impact like headache, gastrointestinal bleeding, kidney and liver failure and cancer. [4, 5] Thus, the elimination of Cu ions from water and wastewater is a significant for protection of the health and environment.

The pollution of water with dyes and metals is a severe problem for the public and the environment. Various industries like textiles, pharmacy, chemicals, coatings industry, metallurgy, pulp and paper, leather, paint, plastics and packaging devour an extensive quantity of chemical reagents and water through dyeing, processing and finishing activities. Dyes and metal ions are general pollutants for water because it is highly soluble. A severity

of ecological problems occurs due to contamination of dyes and metal ions in the environment because it is difficult to degrade by biological methods. The elimination of pollutants like dyes, metals and pigments from wastewater is a significant for water pollution[6].

A variety of procedures have been created for elimination of toxic pollutants from wastewater like ion exchange, flotation membrane filtration, electrochemical treatment, photocatalysis, chemical precipitation,and adsorption.[7,8] Adsorption process is an effective, simple and useful method for of pollutant elimination[9]. Using a suitable adsorbent makes adsorption process suitable, low cost, ease of operation, versatility and an effective method for the elimination of dyes and metals from wastewater. The mainly significant advantages of the adsorbents are the amount of adsorbate that could rise on it.

Nowadays, nanocomposites have been widely used as adsorbent in environmental remediation for metal ions or dye removal with high adsorption capacity due to its suitable pore size, high mechanical strength, ease production, high selectivity and regeneration processes[10]. Recently, polymer-based nanocomposites developed owing to their advantages l film forming ability with variable dimensions and their high functionalities. [11,12] Many polymer nanocomposites have widely utilized for elimination of a variety of toxic dyes, metal ions, and microorganism from water and wastewater for example: magnetic chitosan/Al_2O_3/Fe_3O_4 nanocomposite for removing acid fuchsin dye, [13] titanate layer–natural polymer amylopectin based nanocomposite for adsorption and separation of MB and MO dyes, [14] carboxymethyl-chitosan (CMC)/bentonite composite for adsorption of Cu^{2+} ions, [15] polyaniline/carboxymethyl cellulose/TiO_2 nanocomposites(PAn/CMC/TiO_2) for adsorption of congo red dye, [16] TiO_2-chitosan-polyacrylamide for the uptake of Sirius yellow K-CF dye, [17] TiO_2-Kaolinite nanocomposite for adsorption of Pb(II) and Cd(II) ions, [18]

Several methods used for the preparation of nanocomposite by incorporation of nanomaterials into a polymer through physical blending (mixing), crosslinking and polymerization reactions with monomers, solution casting method, hot press. [19] Gamma radiation is one of the suitable methods for preparation of polymer metal nanocomposite by mixing the metal salt and organic monomer solution. During gamma irradiation and polymerization reaction, a homogeneous dispersion of nanocrystalline metal particles and polymerization of monomer created instantaneously, resulting in formation of in the polymer matrix. Many nanocomposites prepared by gamma radiation for different applications including different metal nanoparticles such as Fe_3O_4. SiO_2, TiO_2, Au, Ag, PbO and Al_2O_3.[20, 21 ,22,23 ,24,25,26]

Radiation is a convenient tool for the cross-linking and modification of polymeric materials without using cross-linking reagent. This technology is environmentally friendly since it leaves no residue or pollutant in the environment.[27]

PVA is a synthetic polymer soluble in water used in various industrial, pharmaceutical, medical, environmental and agricultural applications as a result of its low cost, chemical and physical resistance and amazing film forming property. [28 , 29] Also, acrylamide (AAm) or acrylamide-based polymers is one of the water-soluble polymers that carry a negative charge and named anionic polyelectrolyte and used for a variety of applications in lubrication, effluent reclaiming, mining, Paper manufacture and water management process.[30]

One of the nanomaterials used in removal and adsorption of metals or dyes is to include titanium dioxide. TiO_2 has been widely used owing to its low economic cost and high efficiency in pollution degradation. TiO_2 can be used in many industrial applications like environmental purification, photovoltaic devices, solar energy conversion and optical coating photocatalysis .[31,32]

In this study, gamma radiation synthesize of poly(vinyl alcohol)/polyacrylamide/TiO_2/SiO_2 nanocomposites were obtained by polymerization of PVA and AAm in presence of TiO_2/SiO_2 nanoparticles at different irradiation doses for removal of Cu(II) ions and basic blue 3 dye from their aqueous solutions. The obtained nanocomposites were characterized by FTIR, XRD, SEM, EDS, TEM, and DLS. The batch adsorption experiments by studying the effect of a variety of conditions on dye or metal adsorption in addition to adsorption kinetics, sorption thermodynamic and adsorption isotherm models were also studied.

2. Experimental

2.1. Chemicals

Acrylamide (AAm) 97%, was obtained from Pratap Chemical Industries, India. Poly(vinyl alcohol) (PVA), hydrochloric acid (36.5%), sodium hydroxide was obtained from Qualikemes fine chemicals Pvt. Ltd. New Delhi, India, Nano-sized (10–20 nm) Titanium dioxide (TiO_2) and Silicon dioxide (SiO_2) of purity 99.5% were bought from Sigma Aldrich Chemie. Astrazon blue BG-200% (Basic blue 3), was supplied by Dystar (Cairo, Egypt). NaOH were supplied by Merck Co., Germany.

2.2. Radiation synthesis of PVA-co-AAm and PVA-co-AAm/TiO_2/SiO_2 nanocomposites

Firstly, 10.0 wt% of PVA-co-AAm copolymer was prepared by gamma radiation-induced copolymerization reaction at 30 kGy via mixing of 5wt% of PVA and 5 wt% of AAm solutions. Secondly, sonochemical followed by irradiation copolymerization techniques are used for synthesis of the PVA-co-AAm/TiO_2/SiO_2 nanocomposites as follows: aqueous PVA/AAm solution were prepared by dissolving 4.75 g of PVA in 50 ml of dist. water and 4.75 g of AAm in another 50 ml dist. water under constant stirring at 70 ^oC for 4 h. The two solutions were mixed, stirred and sonicated for 2 h. Then, after complete dissolution of PVA/AAm solution, 0.25 g of TiO_2 and 0.25 g of SiO_2 were added to obtain a reactant mixture of 10 wt%. The reactant mixture stirred for fully dispersion of TiO_2/SiO_2 nanoparticles using ultrasonic (70 w) for 2 h. Finally, after the reaction mixture was homogenized, the reactant mixtures bubbled by nitrogen gas for 5 min, sealed and then polymerization was conducted by exposure to γ-rays (^{60}Co Canadian) irradiation facility at different doses of (10 - 50 kGy) at dose rate of 1.12 kGy/h. The obtained PVA-co-AAm/TiO_2/SiO_2 nanocomposites washed well with ethanol to eliminate unreacted materials, dried at 60 ^oC and then grinded in a mortar to fine powder for further use and analysis.

2.3. The gelation (%)

The dried PVA-co-AAm and PVA-co-AAm/TiO_2/SiO_2 nanocomposites of known weights (W_i) were soaked at 70 ^oC in deionized water for 24 h to eliminate the insoluble parts. Then, dried to a constant weight (W_d). The gelation (%): established according to equation (1):

$$Gelation\ (\%) = \frac{(W_d)}{(W_i)} \times 100 \qquad (1)$$

2.4. Swelling (%):

Known weights (W_d) of dried PVA-co-AAm and PVA-co-AAm/TiO_2/SiO_2 nanocomposites were immersed in dist.water at room temperature until the equilibrium

swelling was obtained after 24h. Then, samples weighed (*Ws*) after removing the excess water on their surfaces by a filter paper. The swelling (%) was estimated according to equation (2):

$$Swelling\ (\%) = \frac{(W_s - W_d)}{(W_d)} \times 100 \qquad (2)$$

2.5. Uptake of basic blue 3 dye or Cu(II) ions

The effect of PVA-co-AAm, PVA-co-AAm/TiO_2/SiO_2 nanocomposites (on adsorption and removal of basic blue 3 dye or Cu(II) ions as adsorbates was studied. Briefly, 0.1 g adsorbent amount was added to 50 ml of aqueous solution of the dye or Cu(II) ions (200 mg/L) at room temperature for 24h with shaking at agitation speed of 100 rpm, then the decrease in UV absorbance was measured to detect the better adsorbent for further batch adsorption experiments. Secondly, the factors affecting the adsorption capacity of basic blue 3 dye or Cu(II) ions onto PVA-co-AAm/TiO_2/SiO_2-30 nanocomposite was examined at varying the experimental conditions by using 50 ml volume of dye or metal ions solution at time intervals up to 24h as follows: (i) the effect of initial concentration (100-250 mg/L), (ii) the effect of adsorbent amount (0.1-0.4 g), (iii) the of effect of pH (4, 7, 9 and 11 for dye; and 3, 4.5 and 6 for Cu(II) ions) and (iv) the effect of temperature at 298, 308 and 318 K. After each experiment, the concentration of dye was determined by measuring its absorption at λ_{max} = 654 nm by using T60 UV/Vis spectrophotometer from PG instruments limited. The remaining Cu(II) ions in the feed solution after adsorption was determined with atomic absorption spectrometer (AAS) - Thermo scientific iCE 3000 series (AA) Spectrometer, Cambridge, England.

The adsorption kinetics, isotherm and thermodynamics study of dye and metal ions were evaluated. The calculation of adsorbed capacity (q_e) at equilibrium and the amount adsorbed (q_t) at time intervals was determined utilizing the following equations:-

$$Amount\ adsorbed(q_e) = \frac{(C_o - C_e) \times V}{m} \qquad (3)$$

$$Amount\ adsorbed(q_t) = \frac{(C_o - C_t) \times V}{m} \qquad (4)$$

The removal (%) was calculated using from equation (5) as follows:

$$Removal\ (\%) = \frac{(C_o - C_e)}{C_o} \times 100 \qquad (5)$$

Where C_0, C_t and C_e are the initial concentrations of dye or metal ions (mg/L) before adsorption, the concentration at time (t) and the concentration at equilibrium, respectively, m is the weight of dry adsorbent (g).; V is the volume of the aqueous dye or metal ions solution (L);

2.6. Characterization Analysis

The chemical structure of the nanocomposites was analyzed by ATR-FTIR spectroscopy, Bruker Optik GmbH, Ettlingen, Germany. XRD-600 instrument with Ni filter and Cu-Kα supplied From Shim Kyoto, Japan, used to obtain X-ray diffraction curves. The surface morphology of the copolymers and nanocomposites was investigated with SEM,

JEOL JSM-5400, Japan.. Energy dispersive spectrometry (EDS) analysis LINK'S (Oxford Instruments link ISIS, UK) connected to scanning electron microscope model JEOL JSM-5400 (Japan) was used to perform the consisting of the peaks belonging to the C, O, Si and Ti. The particle size and distibution examined using a Transmission Electron Microscopy (TEM), JEOL JSM–100 CX, Japan, with an acceleration voltage of 80KV. The distribution of particle of PVA-co-AAm/TiO_2/SiO_2-30 kGy nanocomposite was performed by dynamic light scattering (DLS-ZP/Particle Sizer Nicomp 380ZLS), USA. The effect of nanocomposites on the dye concentration was determined by measuring its absorption at λ_{max} = 654 nm by utilizing the T60 UV/Vis spectrophotometer from PG instruments limited.

3. Results and Discussion

3.1. The effect of irradiation dose on gelation (%) and swelling (%) of PVA-co-AAm / TiO_2/SiO_2 nanocomposites

Gamma irradiation is a useful crosslinking polymerization technique over other chemical cross-qlinker substances and an effective method to make polymeric nanocomposite. In this study, the copolymer prepared at 30 kGy (PVA-co-AAm-30) and three PVA-co-AAm/TiO_2/SiO_2 nanocomposites were prepared using the gamma irradiation technique at different doses of 10, 30 and 50 kGy. Table 1 illustrated the impact of irradiation dose on gelation (%) and swelling (%) of PVA-co-AAm-30 copolymer and PVA-co-AAm/TiO_2/SiO_2 nanocomposites. The increase in irradiation dose from 10 kGy to 50 kGy doses do not lead to significant increase in gelation (%) and it was in the range of 90.8 to 95.7 %. This is due to increasing the cross-linking reaction between PVA-co-AAm upon effect of the gamma irradiation. Also, PVA-co-AAm/TiO_2/SiO_2-30 had the highest swelling (%) of 197.7% then decreases at 50 kGy due to the increase in crosslinking density.

Table 1: **The impact of irradiation dose on gelation (%) and swelling (%) of PVA-co-AAm-30 and PVA-co-AAm/TiO_2/SiO_2 nanocomposites.**

Sample key	Dose (kGy)	Gelation (%)	Swelling (%)
PVA-co-AAm-30	30	89.6	204.3
PVA-co-AAm/TiO_2/SiO_2-10	10	90.8	165.5
PVA-co-AAm/TiO_2/SiO_2-30	30	93.1	197.7
PVA-co-AAm/TiO_2/SiO_2-50	50	95.7	143.6

3.2. Characterization analysis

3.2.1. FT-IR investigation

Figure 1 illustrates the FT-IR spectrum of PVA, AAm and the synthesized kGy nanocomposite. The spectrum of PVA (Figure 1a) demonstrates at 3290 cm^{-1} and 2923 cm^{-1} related to the –OH and C–H alkyl, respectively. Stretching vibration peaks correspond to C–O and C=O from residual ester groups appear at 1427 cm^{-1} and 1728 cm^{-1}, respectively. Also, the stretching vibrations peaks characteristic to C–O and C–O–C appear at 1024 cm^{-1} and 1092 cm^{-1}, respectively.[33]

The FTIR spectrum of AAm Figure 1b shows the peaks at 1603 cm^{-1} and 1656 cm^{-1} corresponding to bending vibration of the $–NH_2$ group and stretching vibrations of the –C=O group, respectively. The peaks at 1421 cm^{-1} and 1467 cm^{-1} resulted from the **scissor**

and bending vibrations of CH-CO and -CH_2 groups, respectively. Additionally, the absorption peak attributed to the stretching vibrations of –CH_2 appear at 2811 cm^{-1}. A broad absorption band resulted from the –NH group appear at 3160 cm^{-1} and 3333 cm^{-1}. Finally, the absorption stretching vibration band from C–N group resulted at 1346 cm^{-1}, while the broad absorption bands resulted from the out of plane bending vibration of NH_2 group appears in the range of 619–655 cm^{-1} were.

The FT-IR spectrum of PVA-co-AAm/TiO_2/SiO_2 nanocomposite. Figure 1c shows stretching vibration peaks characteristic to the C=O of amide I and N–H bending vibration at 1720 cm^{-1} and 1661 cm^{-1}, respectively.[34] Moreover, a minor peak shift and broadening appeared at 3340 cm^{-1} due to the overlapping of -NH groups of AAm and –OH of PVA stretching vibrations forming a hydrogen bonding between them. These results indicated the successful grafting of AAM onto the PVA backbone.[35] The stretching vibration peaks related to the Ti–O–Ti resulted in the range 557-752 cm^{-1}. The stretching vibrations absorption bands resulted from Si-O-Si and Si-O-H appeared at 932 cm^{-1} and 1094 cm^{-1} respectively.

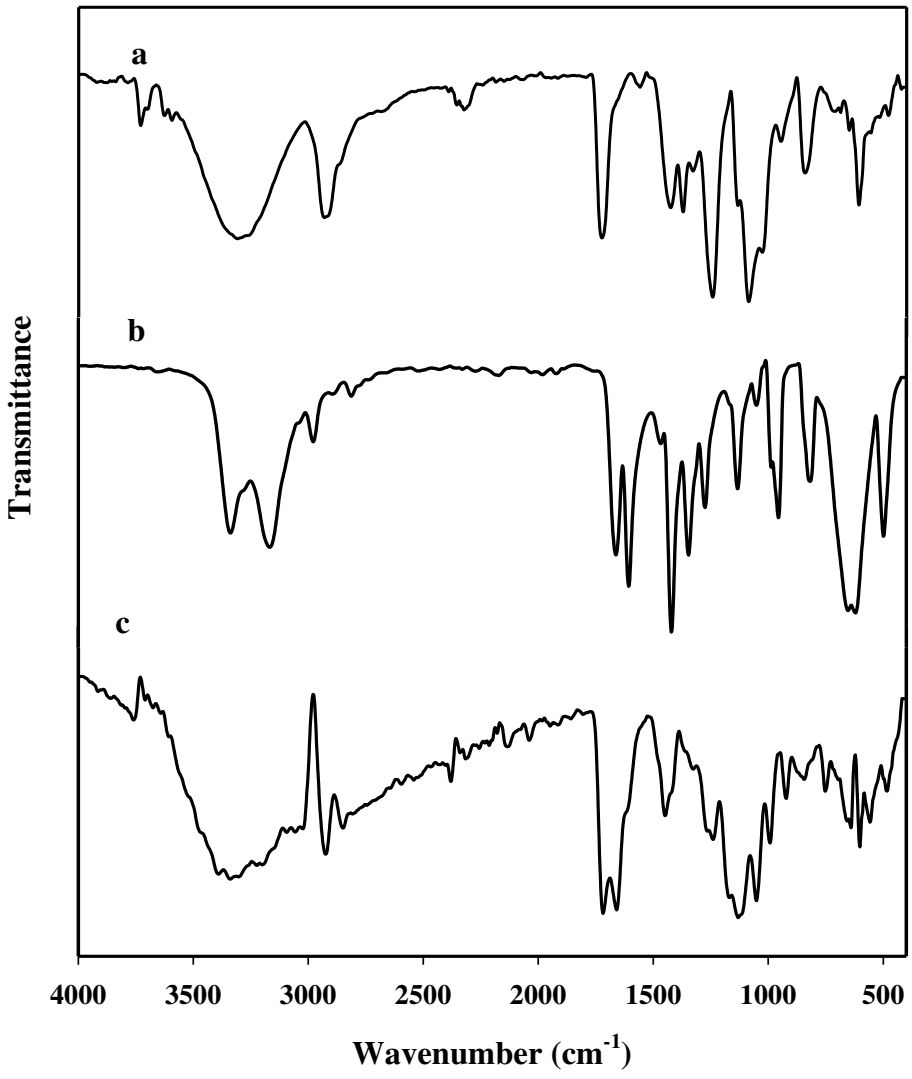

Figure 1:- FTIR spectra of (a) PVA, (b) AAm and (c) PVA-co-AAm/TiO_2/SiO_2 nanocomposite.

3.2.2. XRD studies

X-ray diffraction is an important tool, which provides the crystallinity and lattice structure of nanocomposite. Figure 2 shows the XRD measurements and the crystalline structure of PVA-co-AAm, and PVA-co-AAm/TiO_2/SiO_2 nanocomposites prepared at different doses of 10, 30 and 50 kGy. Figure 2a shows XRD of PVA-co-AAm showed semi-crystalline peaks at the 2θ=19.1°.[36] The XRD curves of PVA-co-AAm/TiO_2/SiO_2 nanocomposite prepared at different doses of 10, 30 and 50 kGy (Figure 2b-d) illustrate the same diffraction peaks of PVA-co-AAm with small shift at 2θ=19.1° which is attributed to the presence of TiO_2 and SiO_2 in addition to the diffraction peak of SiO_2 overlapped with the diffraction peak of PVA-co-AAm at 2θ = 19.1°. The characteristic peaks of TiO_2 nanoparticles observed at 2θ= 25.1°, 37.6 °, 47.9 °, 53.7°, 55.1°, 62.6°, 68.3°, 69.9° and 74.9° which confirms the spinal structure of the Bragg reflections of anatase phase of TiO_2 nanoparticles corresponding to the crystal planes of the (A101), (A004), (A200), (A105), (A211), (A118), (A116) and (A220), respectively. In addition, the peaks at 27°, 36.2° and 55.0° corresponding to the crystal planes of the (R110), (R101) and (R211) which corresponds to TiO_2 in the rutile phase. All peaks are well agreement with the standard spectrum (JCPDS no.: 21-1272, 88-1175 for rutile and 84-1286 for anatase).[37] In the XRD spectra, the characteristic peak at 2θ = 25.10° and 27° signifies the existence of TiO_2, which compatible with the composition of 80% anatase and 20% rutile.[38] The majority structure of TiO_2in anatase phase candidate their possible use as an effective adsorbent for adsorption process of metal ions and dyes.

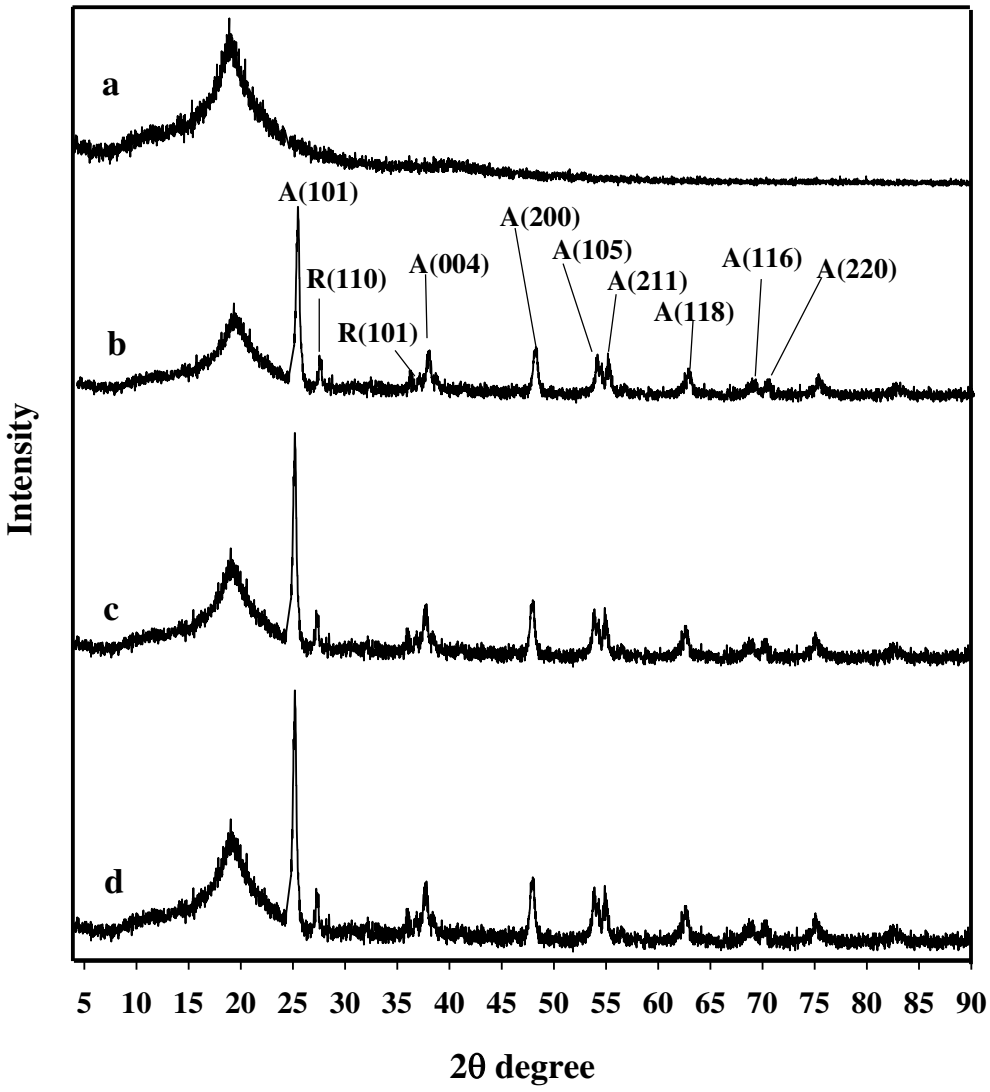

Figure 2:- XRD curves of (a) PVA-co-AAm, (b) PVA-co-AAm/TiO_2/SiO_2-10 (c) PVA-co-AAm/TiO_2/SiO_2-30 and (d) PVA-co-AAm/TiO_2/SiO_2-50 nanocomposites.

3.2.3. TEM and DLS analysis

Figure 3 shows TEM images of PVA-co-AAm/TiO_2/SiO_2 prepared at different irradiation doses of 10, 30 and 50 kGy. Generally, bright images of TiO_2 and SiO_2 nanoparticles with spherical shape embedded in a gray shell of PVA-co-AAm molecules with an average size of 60–70 nm. In addition, the TiO_2 and SiO_2 nanoparticles were dispersed well of good uniform distribution with no agglomeration. It was noticed that the irradiation dose affect TEM results. With increasing the irradiation dose during the preparation of nanocomposite, the high dispersion of TiO_2/SiO_2 nanoparticles inside the nanocomposite especially that prepared at 50 kGy (Figure 3c). The particle size distribution of PVA-co-AAm/TiO_2/SiO_2-30 (Figure 3d) obtained from DLS was homogeneously shape with an average size of about 93.5 nm which is large and nearly close to the TEM characterization due to the association and aggregation molecules of nanocomposite in aqueous media via Vander Waal's force or hydrogen bonding.

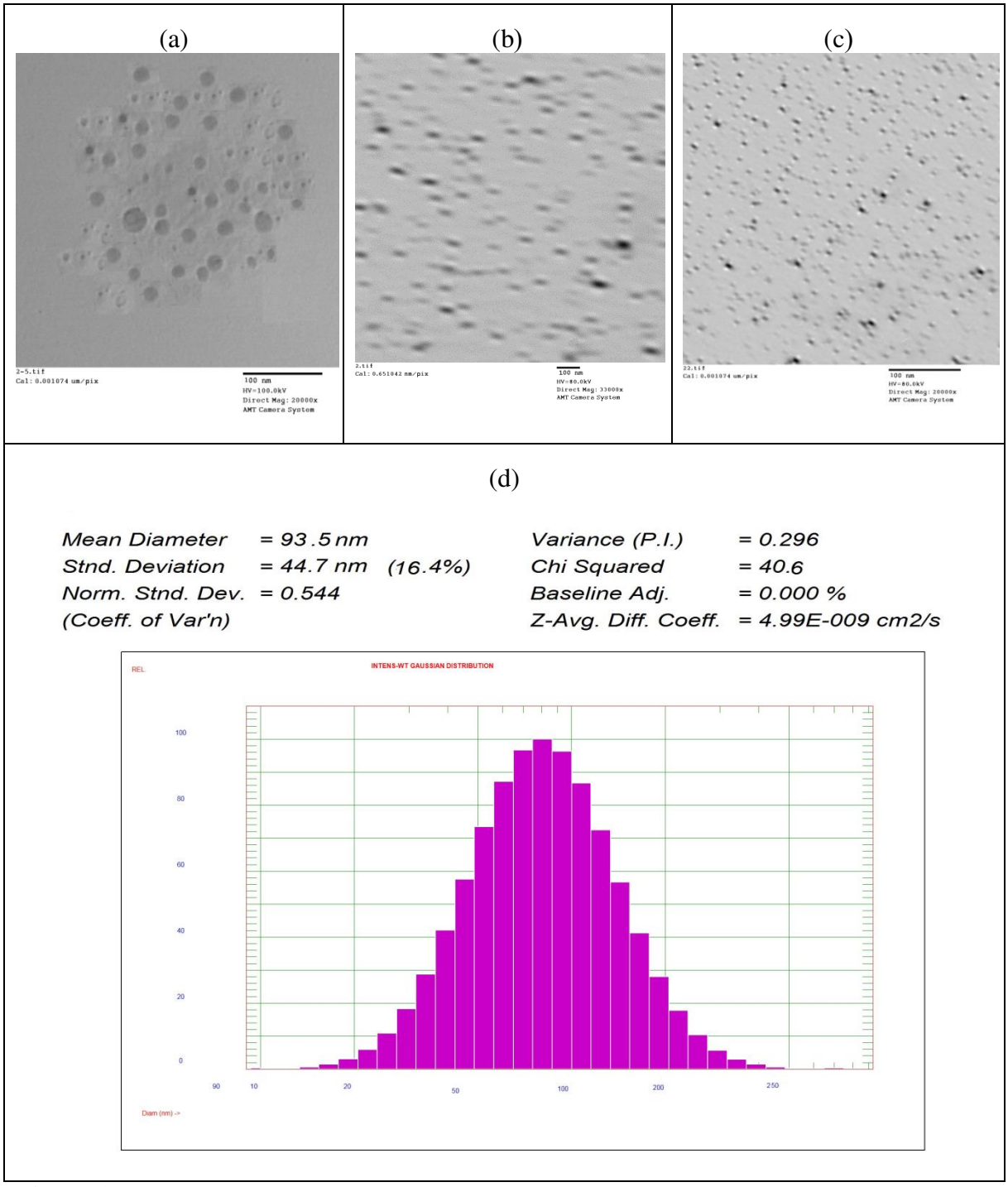

Figure 3:- TEM images of (a) PVA-co-AAm/TiO_2/SiO_2 -10, (b) PVA-co-AAm/TiO_2/SiO_2-30 and (c) PVA-co-AAm/TiO_2/SiO_2-50. (d) DLS of PVA-co-AAm/TiO_2/SiO_2-30 nanocomposite.

3.2.4. SEM and EDX analysis

Figure 4 shows the changes in surface morphology of PVA-co-AAm/TiO_2/SiO_2 nanocomposites investigated by SEM. Figure 4a shows SEM micrograph of PVA-co-AAm/TiO_2/SiO_2-10 had a rocky shape, possess a highly porous structure with white spots and tightly packaged on the back-scattered image seem to be agglomerates particle coated composite surface. While, SEM of PVA-co-AAm/TiO_2/SiO_2-30 (Figure 4b) and PVA-co-AAm/TiO_2/SiO_2-50 (Figure 4c) has coarse surface and in close contact with one another due to increasing the crosslinking of PVA-co-AAm and the formation of semi-interpenetrating crosslinked network. In addition, the TiO_2/SiO_2 nanoparticles well distributed on their surfaces. To confirm the presence of all the mentioned elements including Si, Ti, C and O in the synthesized nanocomposites, elemental analysis was performed on the sample using EDX analysis. Figure 4d demonstrates the EDX analysis of PVA-co-AAm/TiO_2/SiO_2 nanocomposite consisting of the peaks belonging to the C, O, Si and Ti were exactly determined. A mostly intense peak of C is originated from PVA and AAm. O is originated from PVA, AAm, TiO_2, and SiO_2. The result revealed that Ti is detected at 4.5-5.0 KeV and Si is detected at 1.8 KeV.

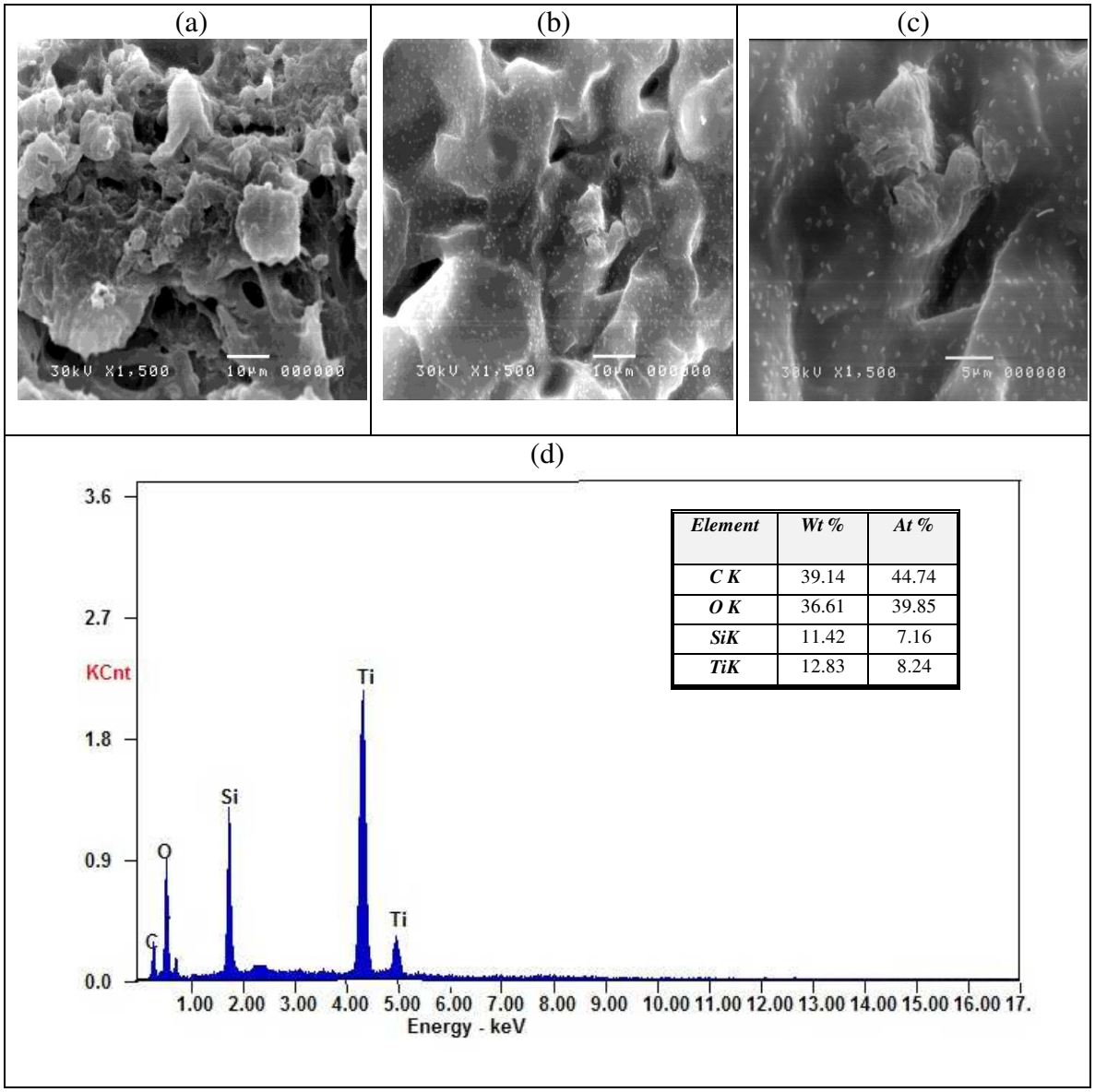

Figure 4: SEM micrographs of(a) PVA-co-AAm/TiO_2/SiO_2-10 (b) PVA-co-AAm/TiO_2/SiO_2-30 and (c) PVA-co-AAm/TiO_2/SiO_2-50.(d) SEM/EDX spectrum of PVA-co-AAm/TiO_2/SiO_2-30 nanocomposite.

3.3. uptake of dye and heavy metal ions

3.3.1. Impact of irradiation dose

Figure 5 shows the UV absorbance of basic blue 3 dye and Cu (II) ions after treatment by PVA-co-AAm and PVA-co-AAm/TiO_2/SiO_2 nanocomposites prepared at different irradiation doses of 10, 30 and 50 kGy. The results show that the PVA-co-AAm/TiO_2/SiO_2 nanocomposites had uptake affinity towards metal ions as well as the dye investigated.

The prepared nanocomposites showed high adsorption capacity compared by PVA-co-AAm. The presence of TiO_2/SiO_2 nanoparticles increases the amount of uptake of dye or Cu(II) 3 folds. Also, the PVA-co-AAm/TiO_2/SiO_2-30 and PVA-co-AAm/TiO_2/SiO_2-50 showed high adsorption capacity. However, PVA-co-AAm/TiO_2/SiO_2-30 shows high swelling (%) as the results obtained from Table 1, and it was selected for further adsorption experiments.

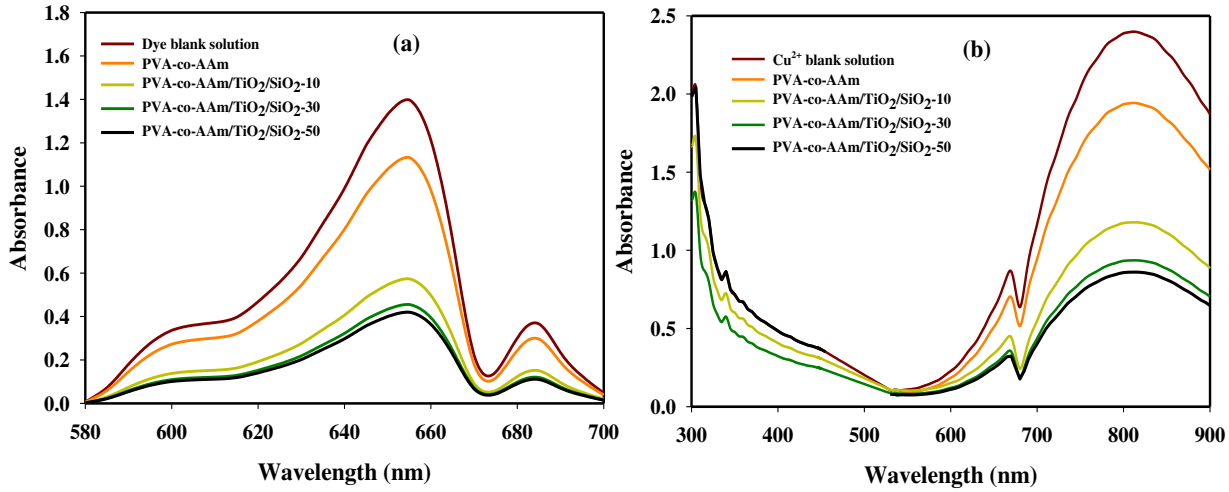

Figure (5): UV absorption spectra of (a) basic blue 3 dye and (b) Cu (II) ions by the effect of the prepared PVA-co-AAm and PVA-co-AAm/TiO_2/SiO_2 nanocomposites.

3.3.2. Effect of pH

The effect of initial pH (4, 7, 9 and 11) and pH (3, 4.5 and 6) on the adsorption capacity and removal (%) of basic blue 3 dye and Cu(II) ions, respectively by PVA-co-AAm/TiO_2/SiO_2-30 nanocomposite as a function of various contact time up to 24 h was investigated in Figure 6.

Generally, the removal (%) of Cu(II) ions and basic blue 3 dye increased as the pH increases. Also, the removal (%) for the adsorbed dye (figure 6a) or Cu(II) ions (Figure 6b) increases as the contact time increases and reaches the equilibrium adsorption after 7h for basic blue 3 dye and 6h for Cu(II) ions. However, as the contact time increased to 24h, the amount of both dye and Cu(II) ions adsorbed onto nanocomposite surface increases slightly. This is owing to the saturation of available surface sites of the nanocomposite. Therefore, the optimized pH for high adsorption noticed at pH 11.0 for basic blue 3 dye and at 6.0 for Cu (II) ions and for the next batch experiments. The removal (%) for basic blue 3 dye and Cu(II) ions was and 83.14 % and 95.42 % at the optimum pH, respectively.

Figure 6b shows that the adsorption of Cu(II) was profoundly dependent on pH, since pH influences the solubility of Cu(II) ions and the ionization state of the -OH and –$CONH_2$ groups in the PVA-co-AAm/TiO_2/SiO_2-30 nanocomposite. In addition, the increase in pH Cu (II) ions (> 6.0) was restricted to avoid the creation of copper hydroxide. The adsorption of the basic blue 3 dye and Cu(II) ions is low at pH < 6. This demonstrates that the solution acidity reduces the basic blue 3 dye and Cu(II) ions adsorption. This behavior could be explained based on change in the surface charge of PVA-co-AAm/TiO_2/SiO_2-30 nanocomposite. In acidic solution, the active groups of PVA-co-AAm/TiO_2/SiO_2-30 nanocomposite such as hydroxyl and amide groups are protonated and competition between H^+ and both basic blue 3 dye and Cu(II) ions for adsorption sites led to little adsorption of metal ion or dye. Meanwhile, as the pH increases, deprotonation of the functional groups occur and the PVA-co-AAm/TiO_2/SiO_2-30 nanocomposite surface charge became negative, which prompted advanced adsorption of cationic species.

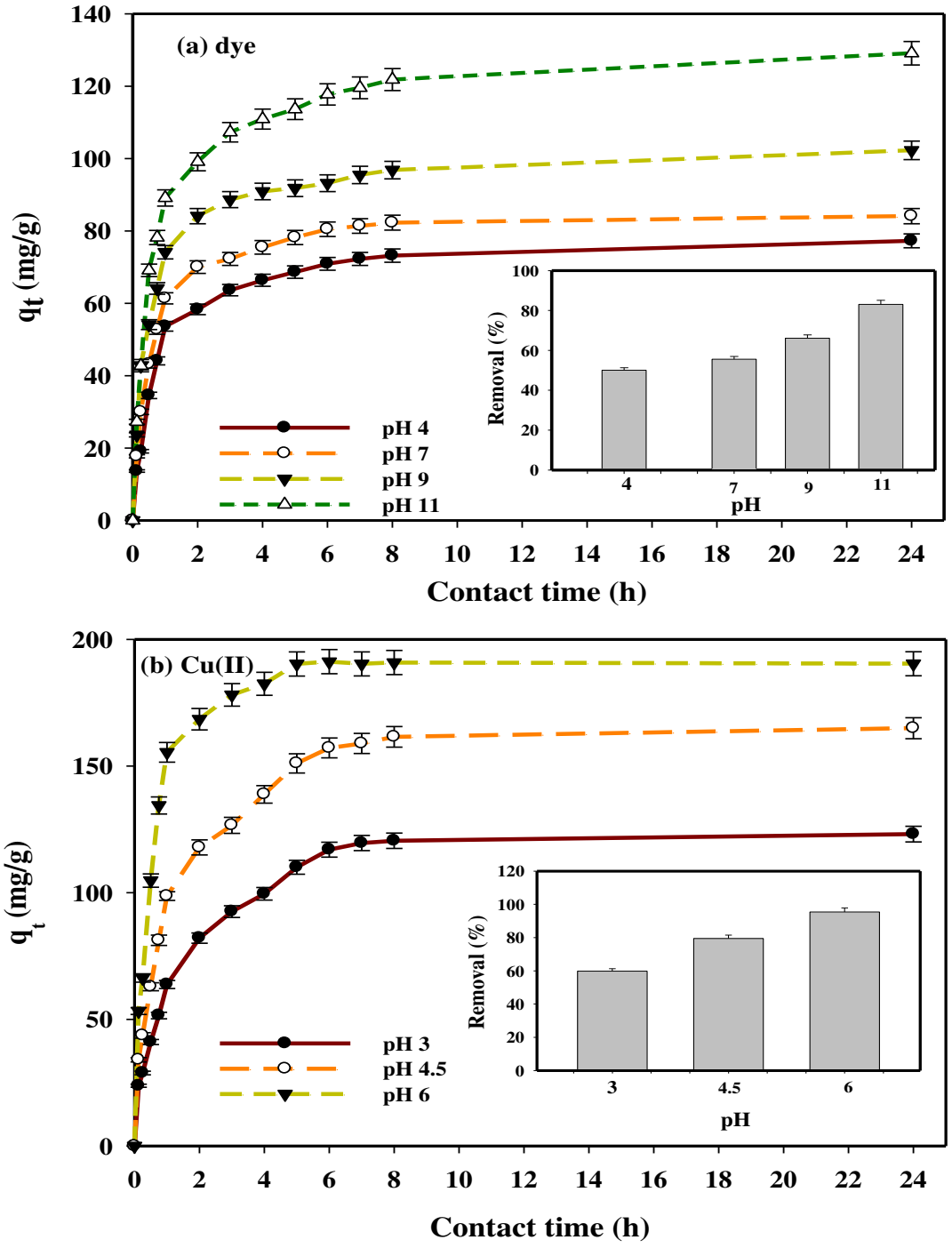

Figure (6): Effect of pH and contact time (h) on the amount adsorbed (q_t) (mg/g) and removal (%) of (a) basic blue 3 dye and (b) Cu (II) ions onto PVA-co-AAm/TiO_2/SiO_2 nanocomposite (initial concentration 150 mg/L for the dye and 200 mg/L for Cu (II) ions; adsorbent dosage 0.3 g; temperature 298 K; agitation speed 100 rpm).

3.3.3. Impact of adsorbent dosage

The impact of PVA-co-AAm/TiO_2/SiO_2-30 nanocomposite dosage (0.1 – 0.4 g) on the amount adsorbed of basic blue 3 dye and Cu(II) ions was considered and the obtained data are presented in Figure 7. The results demonstrate that the removal efficiency (%) regularly increased as the contact time and adsorbent dosage increase and attained the highest values of 93.6% and 98.7% for basic blue 3 dye and Cu(II) ions, respectively with adsorbent dosage 0.3 g of PVA-co-AAm/TiO_2/SiO_2-30 nanocomposite. However, the saturated removal (%) occurred nearly at 0.3 g after contact time nearly 7h for dye and 6h for Cu(II), then extra increase in dosage gives a small increase in basic blue 3 dye or Cu(II)ions adsorption. Thus, 0.3 g of PVA-co-AAm/TiO_2/SiO_2-30 nanocomposite was chosen to be the optimum dosage for the additional adsorption studies. As the adsorbent mass increases, the adsorption increases that attributed to the increased surface area and consequence the availability of more sites for adsorption. Also, as the contact time increases the adsorption capacity increases, designates that the equilibrium adsorption was about (123.9 mg/g and 82.6 Removal %) for basic blue 3 dye and (190.3 mg/g and removal 95.1 %) for Cu (II) ions after about 7 h and 6 h contact time, respectively.

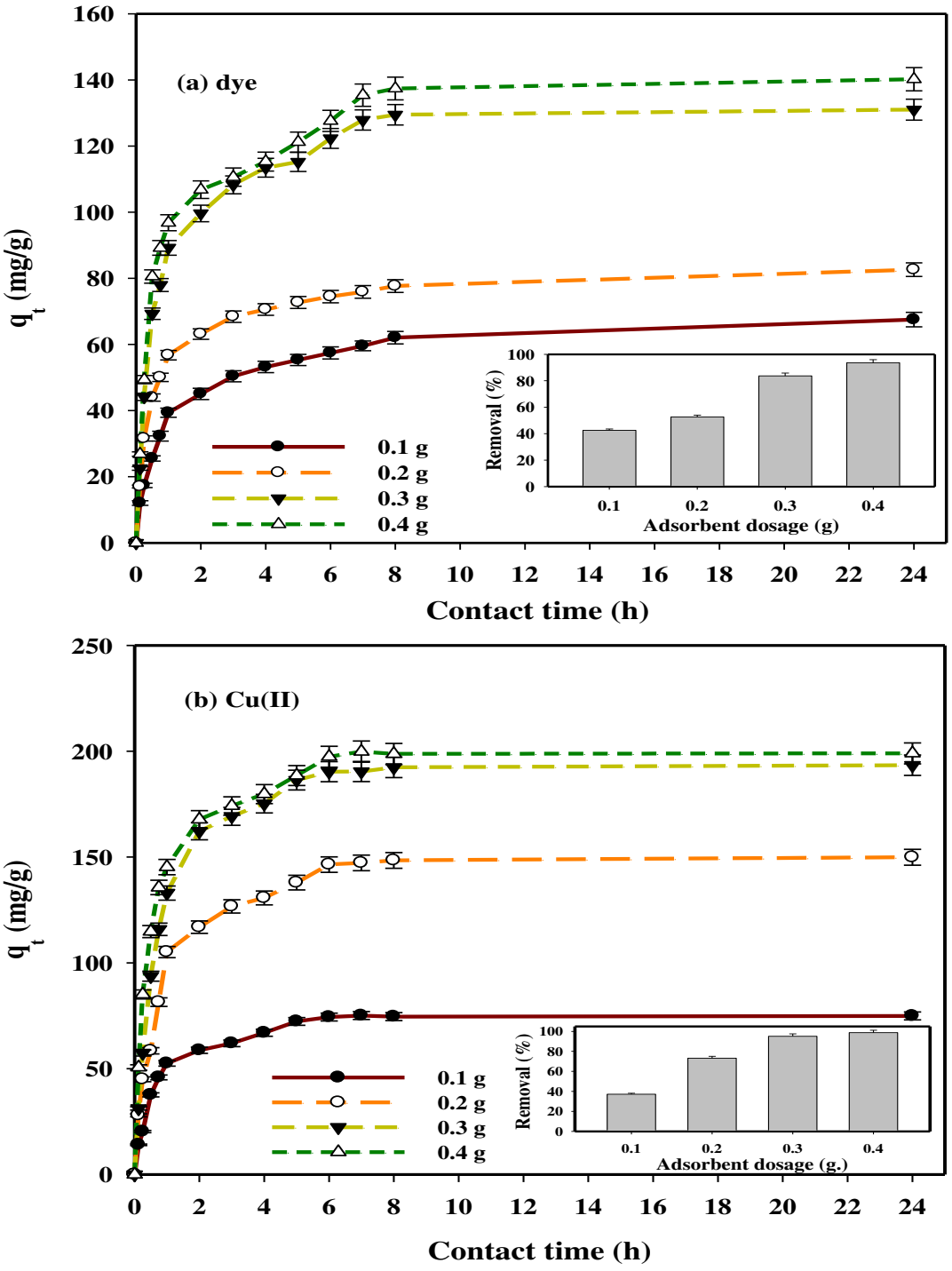

Figure (7): Effect of adsorbent dosages and contact time (h) on the amount adsorbed (mg/g) of the (a) basic blue 3 dye and (b) Cu (II) ions onto the PVA-co-AAm/TiO_2/SiO_2-30 nanocomposite (pH 11 for the dye and pH 6 for Cu (II); initial concentration 150 mg/L for the dye and 200 mg/L for Cu (II) ions; temperature 298 K; agitation speed 100 rpm).

3.3.4. Effect of initial concentration

One of the effective parameters on the adsorption efficiency is the initial concentration of metal ions or dye. The effect of initial concentration (100, 150, 200, and 250 mg/L) of basic blue 3 dye or Cu(II) ions on the adsorption efficiency and removal (%) as a function of various contact times up to 24 h onto the PVA-co-AAm/TiO_2/SiO_2-30 nanocomposite was studied as illustrated in Figure 8.

The results of adsorption demonstrate that the adsorption capacity and the removal (%) of both dye and Cu(II) ions onto the nanocomposite enhanced strongly with the increase in the initial concentration to 150 mg/L for the dye and to 200 mg/L for Cu (II). This enhancement in adsorption efficiency may be because of existing adsorption active sites of PVA-co-AAm/TiO_2/SiO_2-30 nanocomposite are available at low initial concentration, thus resulting in an increase of uptake percentage. At higher concentrations of dye or metal ions, the ratio of the existing surface of nanocomposite to the initial dye or metal ions concentration is minor; consequently, the removal (%) becomes reliant on initial concentrations.[39] However, the adsorption capacity (mg/g) of the dye or the metal ions increased with increasing their initial concentrations. The maximum adsorption capacity of basic blue 3 dye and Cu (II) ions noticed at 123.9 and 190.3 mg/g, respectively. From the acquired outcomes, it was apparent that PVA-co-AAm/TiO_2/SiO_2-30 nanocomposite exhibited strong affinity towards Cu (II) ions than dye. This is because of the variation in the charge density and the size of the dye and Cu(II) ions. Cu (II) ions have greater charge density and smaller size rather than the dye and have a strong attraction to the oxygen and nitrogen atoms lone pair electrons in the hydroxyl and amide groups of nanocomposite forming stable complexes.

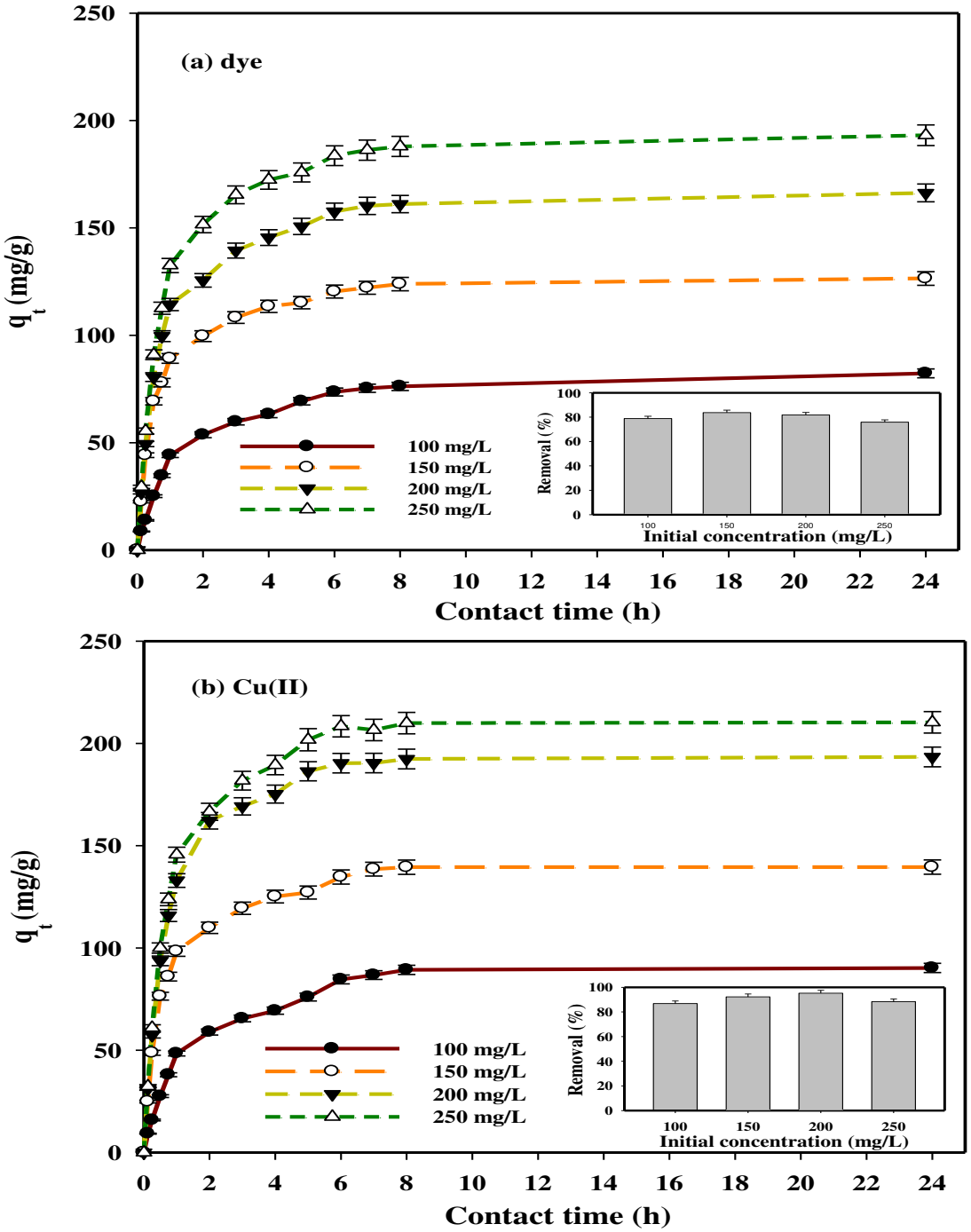

Figure (8):- Impact of initial concentration (mg/l) with contact time (h) onto the amount adsorbed (mg/g) and removal (%) of the (a) basic blue 3 dye and (b) Cu (II) ions onto the PVA-co-AAm/TiO_2/SiO_2-30 nanocomposite (pH 11 for the dye and pH 6 for Cu (II), 0.3 g adsorbent dosage. temperature 298 K; agitation speed 100 rpm).

3.3.5. Impact of temperature

Temperature is a significant factor in the strategy of dye or metal ions adsorption and considered as an important factor to study their thermodynamic behaviors to detect whether the adsorption performance is an exothermic or endothermic reaction. Figure 9 represents the relationship between the temperature dependence and the amount adsorbed (mg/g) or removal (%) of the basic blue 3 dye and Cu (II) ions and onto the PVA-co-AAm/TiO_2/SiO_2-30 nanocomposite was performed at 298, 308 and 318 K. It is noticed that the amount of adsorption (mg/g) and removal (%) of both dye and metal ions increases with increasing temperature from 298 to 318 K. The adsorption capacities of the prepared nanocomposite on the dye increased from 117.1 to 123.9 mg/g for the dye and increased from 190.3 to 196.6 mg/g for Cu (II) ions. This is attributed to the increment in the kinetic energy of the adsorbent molecules with the increment in temperature, the increased activated sites created on the PVA-co-AAm/TiO_2/SiO_2-30 nanocomposite and the increase in kinetic motion of metal ion molecules that leads to increase the penetration of metal ions inside the micropores of the prepared nanocomposite as temperature increased. Also, with increasing the temperature, the speed of diffusion of dye molecules through the exterior boundary layer and in the interior holes in the nanocomposite increases with the temperature and the amount of the adsorbed Cu(II) ions or the dye adsorption increases. The results revealed that the adsorption process is an endothermic reaction and prepared nanocomposite is a successful adsorbent for the adsorption of basic blue 3 dye or Cu (II) ions from wastewater.

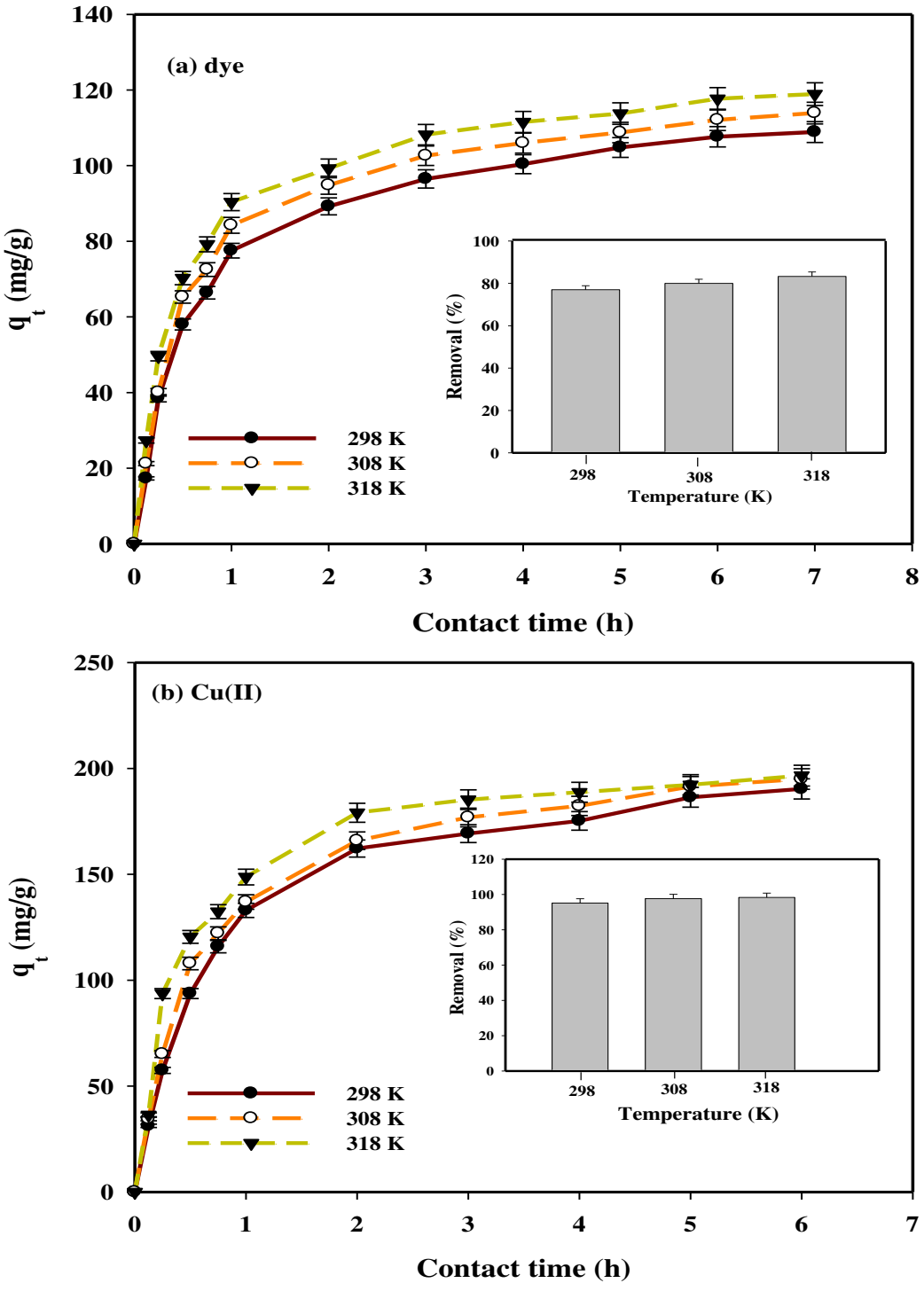

Figure (9):- Impact of temperature (K) with contact time (h) onto the amount adsorbed (mg/g) and removal (%) of the (a) basic blue 3 dye and (b) Cu (II) ions onto PVA-co-AAm/TiO_2/SiO_2-30 nanocomposite (pH11 for the dye and pH 6 for Cu (II) ions; contact time 7h for the dye and 6 h for Cu (II); 0.3 g adsorbent dosage; initial concentration 150 mg/L for the dye and 200 mg/L for Cu (II) ions; agitation speed 100 rpm).

3.3.6. Sorption isotherms.

The sorption isotherm examines are significance in deciding the adsorption capacity of the PVA-co-AAm/TiO_2/SiO_2 -30 nanocomposite to identify the character of adsorption. Langmuir, Freundlich and Temkin isotherm models were used to fit the experimental data of the adsorption isotherm.

The Langmuir isotherm supposes that adsorption sites are energetically equivalent, indistinguishable and just monolayer adsorption takes place in the procedure.[40] The Langmuir equation is expressed by equation (6):

$$\frac{C_e}{q_e} = \frac{1}{q_m K_L} + \frac{C_e}{q_m} \qquad (6)$$

Where, q_e (mg/g) is the adsorption capacity at equilibrium, q_m (mg/g) is the maximum adsorption capacity, C_e is the concentration of dye after adsorption (mg/L). K_L and K_F are the Langmuir and Freundlich constant, respectively; n is related to the adsorption intensity. K_L (L/g) and q_m of Langmuir isotherm obtained by plotting the curve C_e/q_e versus C_e.

Also, The favorability of PVA-co-AAm/TiO_2/SiO_2-30 nanocomposite as an adsorbent for basic blue 3 dye and Cu (II) ions Langmuir adsorption constant K_L and can be represented in terms of the Langmuir isotherm is R_L which is a dimensionless separation. R_L can be calculated using equation (7) that describes the adsorption process whether favorable or unfavorable. R_L value is between 0-1. If $R_L > 1$ suggesting the adsorption is unfavorable, if $R_L = 1$ suggesting the adsorption is linear, if $0 < R_L < 1$ suggesting the adsorption is favorable and if R_L equals 0, it represents irreversible adsorption

$$R_L = \frac{1}{1 + K_L C_o} \qquad (7)$$

The Freundlich model is an experimental equation utilized to express the multilayer adsorption on a heterogeneous surface[41] and described by equation (8).

$$\ln q_e = \ln K_F + \frac{1}{n} \ln C_e \qquad (8)$$

Meanwhile, K_F is Freundlich isotherm constant [$(mg.g^{-1})(L.mg^{-1})^{1/n}$] (L/g) obtained by plotting the curve $ln\ q_e$ versus $ln\ C_e$ and n is (dimensionless) the heterogeneity factor associated with the adsorption intensity and adsorption capacity.

The Temkin isotherm model supposes that the adsorption heat of all molecules reduces linearly with the enhanced in coverage of the adsorbent surface, the adsorption is described by a homogeneous distribution up to the highest binding energy. The Temkin isotherm can be illustrated by Equation (9).

$$q_e = \frac{RT}{b_T} \ln K_T + \frac{RT}{b_T} \ln C_e \quad , \qquad B = \frac{RT}{b_T} \qquad (9)$$

Where K_T is the equilibrium-binding constant ($L.mg^{-1}$) related to the maximum binding energy, B is corresponding to the adsorption heat, T is the temperature (K) and R is the universal gas constant (8.314 J/K.mol).

Figure 10 shows the experimental Langmuir, Freundlich and Temkin isotherms plots for the removal of basic blue 3 dye or Cu (II) ions solution onto PVA-co-AAm/TiO_2/SiO_2-30 nanocomposite at temperature 298ºK. The resulted correlation coefficients $R^2$and the isotherm parameters (K_L, K_F, K_T, q_m, n) are scheduled in Table 2.

The Langmuir model has the much closed to unity R^2 value than the other two isotherms. This corroborates the adsorption process is a monolayer onto PVA-co-AAm/TiO_2/SiO_2-30 nanocomposite. The theoretical monolayer capacities of PVA-co-AAm/TiO_2/SiO_2-30 nanocomposite ($q_{m,cal}$) for basic blue 3 dye and Cu (II) ions were also got closer to the experimentally resulted value (Table 2).

Table 2 presents the calculated R_L values in the range of 0.0023-0.58111 and 0.377-0.936 for dye and Cu(II) ions adsorption. R_L is lower than 1 ($0 < R_L < 1$) indicates that PVA-co-AAm/TiO_2/SiO_2-30 nanocomposite is a good medium for the adsorption of chosen dye and Cu (II) ions. Also, the outcomes in Table 2 designate that the equilibrium results is not fitted to the Temkin or Freundlich isotherm model.

The adsorption capacity (q_m) of basic blue 3 dye and Cu (II) ions onto PVA-co-AAm/TiO_2/SiO_2-30 nanocomposite were compared with the other adsorbents as represented in Table 3. It is apparent that PVA-co-AAm/TiO_2/SiO_2-30 nanocomposite has a good adsorption capacity comparing with other adsorbents. Consequently, the prepared nanocomposite has a good potential for the adsorption of the dyes and heavy metal ions from aqueous solutions.

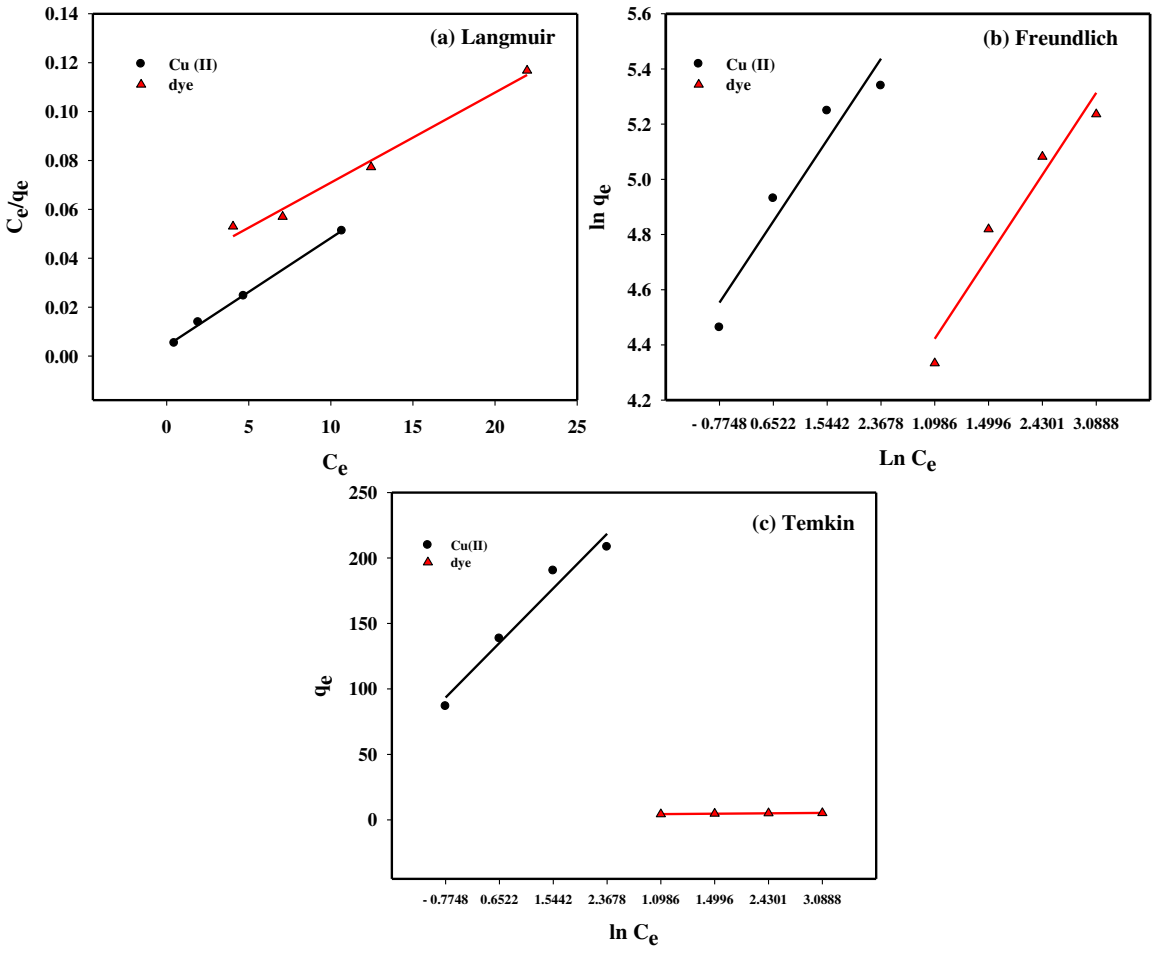

Figure (10):- (a) Langmuir, (b) Freundlich and (c) Temkin isotherm for adsorption of basic blue 3 dye and Cu (II) ions onto PVA-co-AAm/TiO_2/SiO_2-30 nanocomposite.

Table 2:- The Langmuir, Freundlish and Temkin isotherms and correlation coefficients parameters for adsorption of basic blue 3 dye and Cu(II) ions onto PVA-co-AAm/TiO_2/SiO_2-30 nanocomposites.

Adsorbate	$q_{e,exp}$	Langmuir isotherm				Freundlish isotherm			Temkin isotherm			
	(mg/g)	$q_{e,cal}$ (mg/g)	K_L(L/ mg) x 10^{-3}	R_L	R^2	K_F (mg.g^{-1}) (L.mg^{-1})$^{1/n}$	n	R^2	B (10^{-5} L mg^{-1})	K_T	b_T L/g	R^2
Basic blue 3	123.86	171.37	1.711	0.0023 - 0.5811	0.9857	56.43	2.432	0.8752	4. 11	18.27	60.28	0.8752
Cu(II) ions	190.3	226.6	1.058	0.377 - 0.936	0.998	122.49	4.175	0.919	4.98	17.25	60.45	0.9393

Table (3):- comparative study between PVA-co-AAm/TiO_2/SiO_2-30 nanocomposite with other adsorbents in the literature used for wastewater treatment.

Adsorbent	adsorbate	Adsorption capacity (mg/g)	kinetic model	Isotherm model	Ref.
polyaniline/ carboxymethyl cellulose/TiO_2 nanocomposites	Congo Red dye	94.28	Pseudo-second order model	Langmuir isotherm model	[42]
Chitosan/tripolyphosphate/ TiO_2 nanocomposite	orange 16 dye	618.7	Pseudo-second order model	Freundlich model	[43]
phosphorylated polyhydroxyethyl methacrylate hydrogel	Cu (II) ions	66.3	Pseudo-second order model	Langmuir isotherm model	[44]
Carboxymethyl-chitosan / bentonite composite	Cu (II) ions	81.4	Pseudo-second order model	Langmuir isotherm model	[45]
hydroxyapatite/biochar nanocomposites	Cu (II) ions	99.01 mg/g	Pseudo-second order model	Langmuir isotherm model	[46]
PVA-co-AAm/TiO_2/SiO_2-30 nanocomposite	Cu (II) ions	190.3	Pseudo second order	Langmuir isotherm model	This study
	Basic blue 3 dye	123.8	Pseudo second order	Langmuir isotherm model	This study

3.3.7. Sorption kinetics

The studies of the adsorption kinetics play a critical function for estimating the optimal conditions for an adsorption process in order to evaluate the adsorbent features. This is because the adsorption capacity is an important parameter for determination the adsorbed amount of the pollutants (dye or metal ions) by the adsorbent. Thus, several kinetics adsorption models were modulated to assess the experimental data and to best fit the kinetics for the adsorption mechanism process of the basic blue 3 dye or Cu(II) on PVA-co-AAm/TiO_2/SiO_2-30 nanocomposite. Among of them (i) the pseudo first order model as applied in Equation 10 (the most dependable kinetics equation appropriate merely for the quick initial phase), (ii) the pseudo second order model (for expecting the kinetic performance of chemical sorption as a rate controlling advance) expressed by Equation 11 and (iii) the intra-particle diffusion equation (supposes that the mass transfer resistance influence the binding of the contamination to the adsorbent surface) as expressed in Equation 12.

The pseudo-first-order proposed by Lagergren and Svenska **1898** [47] as presented by equation (10)

$$\ln(q_e - q_t) = \ln q_{e1,cal} - K_1 t \qquad (10)$$

The pseudo-second-order kinetics model[48] is presented by equation (11):

$$\frac{t}{q_t} = \frac{1}{k_2 {q_{e2,cal}}^2} + \frac{t}{q_{e2,cal}} (11)$$

q_e, $q_{e,cal}$ and q_t are the experimental, calculated and the adsorbed amount of the dye or Cu (II) (mg/g) at time t (min), respectively. K_1 (min^{-1}) and K_2 (g mg^{-1} min^{-1}) are the pseudo first order and the pseudo second order rate constants, respectively. The linear plots of the curve *ln* (q_e - q_t) versus *time (min)* were used to calculate the values of the rate constant (K_1), meanwhile, (t/q_t) versus *time (min)* was used to calculate the values of the rate constant (K_2).

The intra-particle diffusion equation

$$q_t = k_{id} t^{0.5} + C \qquad (12)$$

where k_{id} (mg. g^{-1}.$min^{-0.5}$) is the intra-particle diffusion rate constant.

The experimental results fitted to the kinetics models revealed above. The pseudo first order constants k_1, $q_{e1,cal}$ and R^2 for the studied basic blue 3 dye or Cu (II) ions adsorption onto PVA-co-AAm/TiO_2/SiO_2-30 nanocomposite are represented in Figure 11 and Table 4. The theoretical q_e quantity calculated from the first order kinetic model ($q_{e1,cal}$) disagree with the practical quantity ($q_{e,exp}$), and the correlation coefficients was likewise established to be marginally lower. These outcomes represented that the pseudo first order kinetic model was not fitting for the adsorption of tested adsorbates.

As indicated by the outcomes recorded in **Table 4**, the estimations of R^2 for the pseudo second order kinetic model were a lot nearer to unity for the adsorbent PVA-co-AAm/TiO_2/SiO_2-30 nanocomposite. The intra-particle diffusion model represented a helpless fit to the practical data, meaning that the intra-particle diffusion was not the rate determining step in the adsorption. The adsorption capacities determined from the pseudo second order model $q_{e2,cal}$ were likewise near to those obtained by experiments ($q_{e,exp}$). The pseudo second order model is depends on the hypothesis that the rate-deciding step might be a chemical sorption including valence powers via exchange or sharing of electrons between the adsorbate and the adsorbent [49,50]. The n and K_2 data determined from the pseudo second order kinetic model were higher for Cu (II)ions than basic blue 3 dye. Among the mentioned models, pseudo second order is suitable model for fitting the adsorption process.

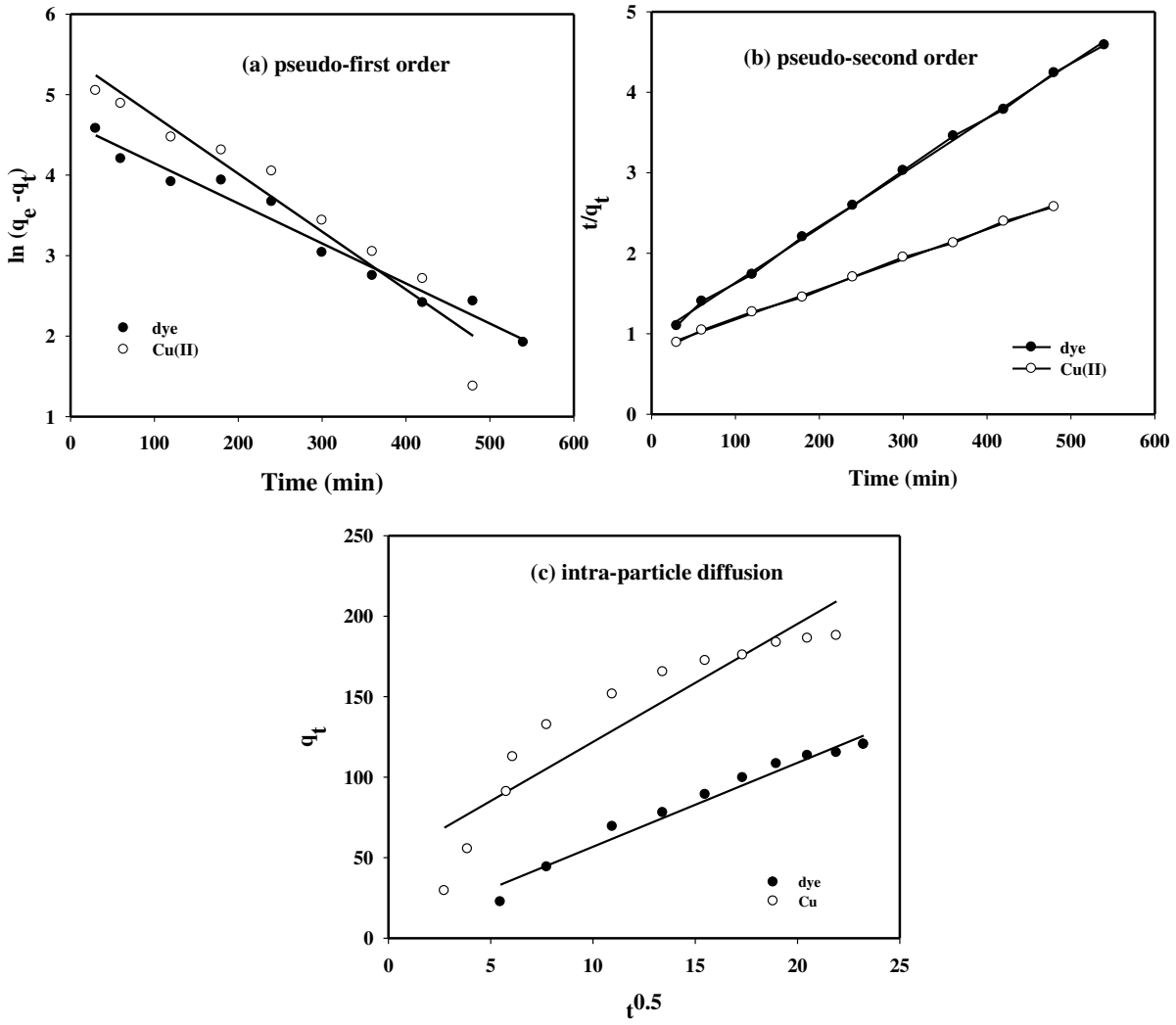

Figure (11):- plots of (a) pseudo first order, (b) pseudo second order and (c) intra-particle diffusion kinetic models applied for adsorption of basic blue 3 dye and Cu(II) ions onto PVA-co-AAm/TiO_2/SiO_2-30 nanocomposite.

Table 4:- Kinetic parameters and correlation coefficients of for adsorption of basic blue 3 dye and Cu (II) ions onto PVA-co-AAm/TiO_2/SiO_2-30 nanocomposite .

adsorbate	$q_{e,exp}$	Pseudo first order	Pseudo second order	Intra-particle diffusion

	(mg/g)							model		
		K_1 (10^{-3} min^{-1})	$q_{e,cal}$ (mg/g)	R^2	K_2 (10^{-2} g.mg^{-1}.min^{-1})	$q_{e,cal}$ (mg/g)	R^2	k_{ip} (mg. g^{-1}. $min^{-0.5}$)	C_i	R^2
Dye	123.9	4.975	201.01	0.9716	4.878	146.7	0.9990	7.333	40.852	0.8527
Cu(II)	190.3	7.194	233.9	0.9360	2.733	213.4	0.9986	5.213	4.649	0.9702

3.3.8. Adsorption thermodynamics.

To describe the adsorption of basic blue 3 dye and Cu (II) ions onto PVA-co-AAm/TiO_2/SiO_2-30 nanocomposite anyway the procedure is spontaneous or non-spontaneous, the thermodynamic parameters, for example, standard enthalpy change (ΔH^0), Gibbs free energy change (ΔG^0) and standard entropy change (ΔS^0) were calculated to recognize better the impact of the temperature on the adsorption process. The equilibrium constant K was used to calculate the Gibbs free energy (ΔG^0) as in equation (13) where, R is gas constant (8.314 J/mol.K), T is the temperature in Kelvin (K),

$$\Delta G^o = -RT \ln k \qquad (13)$$

Additional thermodynamic parameters, such as enthalpy change (ΔH^o) and entropy change (ΔS^o), were calculated from equation (14)[51] and illustrated in Figure 12:

$$\ln k = \ln\left(\frac{q_e}{C_e}\right) = \frac{\Delta S^o}{R} - \frac{\Delta H^o}{RT} \qquad (14)$$

$\Delta H°$ and $\Delta S°$ were determined from (Figure 12) from the slope and intercept value of the linear plot of $ln\ (q_e/C_e)$ versus $1/T$. The obtained data are listed in **Table 5.** ΔG^0 values established here are negative for adsorption of the dye and the Cu (II) onto the nanocomposite. This demonstrates that the adsorption procedure is spontaneous and thermodynamically practicable. Furthermore, the ΔG^0 values decreased as the temperature increased, demonstrating an increased tendency in the degree of practicability and spontaneity of uptake of the dye or metal ions onto PVA-co-AAm/TiO_2/SiO_2-30 nanocomposite. The adsorption enthalpy change (ΔH^0) was determined to be 35.97 kJ/mol for Cu (II) and 31.13 kJ/mol for the basic blue 3 dye adsorption onto PVA-co-AAm/TiO_2/SiO_2-30 nanocomposite, respectively. The positive change in enthalpy proposes that this adsorption is chemisorption. Additionally, positive ΔS^0 indicates an irregular raise of the randomness at the nanocomposite-solution interface through adsorption.

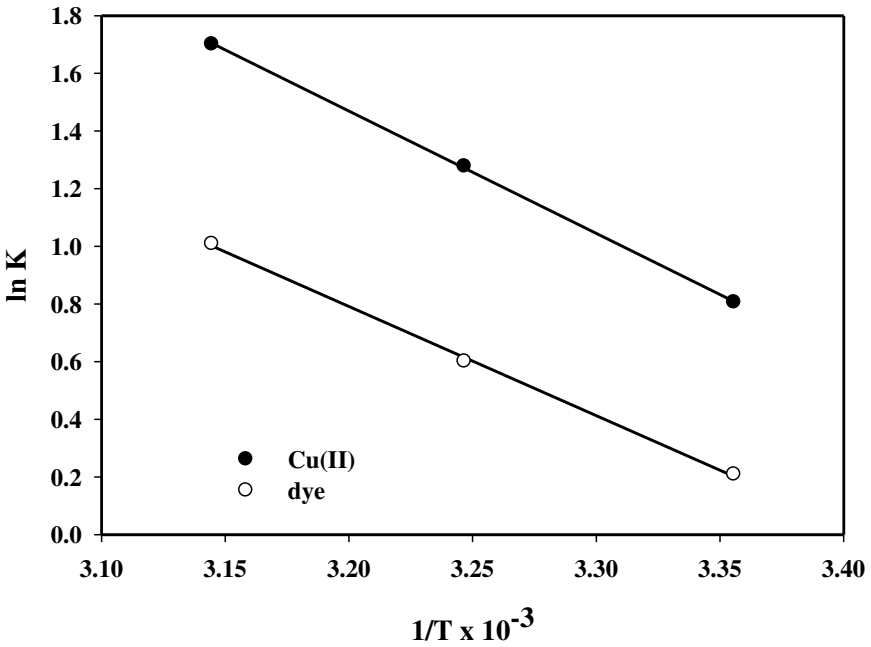

Figure (12):-Van't Hoff plots of the Cu (II) ions and basic blue 3 dye adsorption at different temperatures (50 ml of initial concentration 150 mg/l for the dye and 200 mg/l for Cu(II) ions; 0.3 g adsorbent dosage, pH 6 for Cu (II) and pH 11 for the dye; contact time 6 h for Cu (II) and 7 h for the dye).

Table 5:- Thermodynamic parameters at different temperatures

adsorbate	Standard enthalpy ΔH^o (kJ.mol^{-1})	Standard entropy ΔS^o (J.mol^{-1}.K^{-1})	Gibbs free energy ΔG^o (kJ.mol^{-1})		
			298 K	308 K	318 K
Basic blue 3	31.132	10.51	- 31.024	- 33.104	- 34.241
Cu (II) ion	35.965	13.11	- 38.013	- 40.937	- 41.985

3.3.9. Reuse of adsorbents.

The reuse of adsorbents after a particular procedure is perhaps the main significant properties for economic and environmental reasons. Thus, the desorption–adsorption series were carried out to examine the capability of PVA-co-AAm/TiO_2/SiO_2-30 nanocomposite for application. In this work, ethanol and sodium hydroxide (alkaline environment 0.1 M) solution were utilized as desorption medium for basic blue 3 dye. Desorption of adsorbed Cu(II), was done utilizing nitric acid solution and the reusability was assessed four times as demonstrated in figure 13. It was established from this figure that adsorption of Cu(II) or basic blue 3 dye was very little influenced. In this manner, PVA-co-AAm/TiO_2/SiO_2-30 nanocomposite can be utilized many times for water contamination remediation.

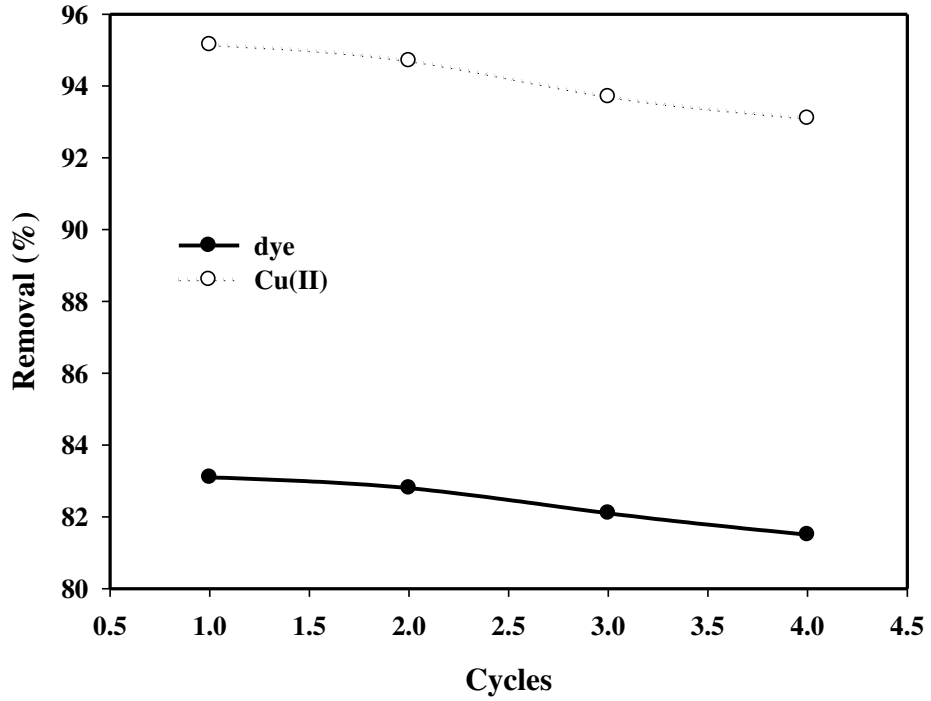

Figure 13: effect of cycle times on removal (%) of basic blue 3 dye and Cu(II) onto PVA-co-AAm/TiO_2/SiO_2-30 nanocomposite

4. Conclusion

Novel PVA-co-AAm/TiO_2/SiO_2 nanocomposites prepared by γ-irradiation polymerization crosslinking of PVA and AAm incorporated with TiO_2/SiO_2 nanoparticles. The highest and equilibrium swelling (%) of the prepared nanocomposites was noticed at 30 kGy. The chemical structure of the prepared nanocomposites was an;lyzed by FT-IR, XRD, EDS, SEM, TEM and DLS. The adsorption capacity of PVA-co-AAm/TiO_2/SiO_2 nanocomposites towards basic blue 3 dye and Cu(II) ions was studied. The prepared nanocomposites at different doses showed high adsorption capacity 3 folds compared by PVA-co-AAm adsorbent. The PVA-co-AAm/TiO_2/SiO_2-30 shows high swelling (%) as well as high adsorption and removal (%) towards the tested dye and metal ions. The optimum adsorption capacity (mg/g) and removal (%) of basic blue 3 dye or Cu(II) ions from their aqueous solutions onto PVA-co-AAm/TiO_2/SiO_2 nanocomposites were dependent on irradiation of cross-linking, pH, temperature, initial of dye or metal concentration, type of and contact time. The equilibrium adsorption for basic blue dye was about 123.9 mg/g with Removal of 82.6 % at 7h contact time, pH 11, adsorbent dosage 0.3 and initial concentration 150 mg/L. Also, The equilibrium adsorption for Cu(II) ions was about 190.3 mg/g with Removal of 95.1 % at 6h, pH 6, adsorbent dosage 0.3 g and initial concentration 200 mg/L. The adsorption kinetics suggested that the adsorption of each of the dye or Cu(II) ions on the nanocomposite best agree with the Pseudo second order model. The adsorption isotherm results confirmed that the adsorption were fitted to the Langmuir adsorption. The thermodynamic study confirmed that the chemi-sorption

procedure was spontaneous and endothermic. Therefore, the radiation prepared PVA-co-AAm/TiO_2/SiO_2 nanocomposite could be applied as an efficient and novel adsorbent for elimination of dyes and metal cations from contaminated water with high adsorption capacity and convenient recovery.

Ethical approval
Not applicable.

Consent to participate
Not applicable.

Consent to publish
Not applicable. All authors approved for publication.

Author's contributions
Ahmed M.Elbarbary was responsible for the conception and design, testing, data acquisition, writing - review, and editing. **Yasser H.Gad** was responsible for analysis and data interpretation, writing - review, and editing manuscript. All authors read, revise, and approved the final manuscript.

Funding
Not applicable.

Data availability statement
The data that support the findings of this study are available from the corresponding author upon reasonable request.

Conflict of interest
The authors declare that they have no competing interests and non-financial competing interests.

ORCHID
Ahmed M. Elbarbary: https://orcid.org/0000-0001-5318-602X
Yasser H. Gad: https://orcid.org/0000-0002-6973-0701

References

[1] Vareda, J.P.; Valente, A.J.M.; Durães, L. Assessment of heavy metal pollution from anthropogenic activities and remediation strategies: A review.*J. Environ. Manag.***2019**, *246*, 101–118.

[2] Ahmad, Z.; Gao, B.; Mosa, A.; Yu, H.; Yin, X.; Bashir, A.; Ghoveisi, H.; Wang, S. Removal of Cu(II), Cd(II) and Pb(II) ions from aqueous solutions by biochars derived from potassium-rich biomass. *J. Clean. Prod.***2018**, *180*, 437–449.

[3] Akar, S.T.; Akar, T.; Kaynak, Z.; Anilan, B.; Cabuk, A.; Tabak, Ö.; Demir, T.A.; Gedikbey, T. Removal of copper(II) ions from synthetic solution and real wastewater by

the combined action of dried Trametesversicolor cells and montmorillonite. *Hydrometallurgy* **2009**, *97*, 98–104.

[4]Uddin, M. K. (2017). A review on the adsorption of heavy metals by clay minerals, with special focus on the past decade. *Chemical Engineering Journal*, *308*, 438-462

[5] Basri, S. N., Zainuddin, N., Hashim, K., &Yusof, N. A. (2016).Preparation and characterization of irradiated carboxymethyl sago starch-acid hydrogel and its application as metal scavenger in aqueous solution. *Carbohydrate polymers*, *138*, 34-40.

[6]Khalaf MN (ed) (2016) Green polymers and environmental pollution control. CRC Press; Apple Academic Press Inc, Oakville, p 436.

[7]Tanan, W., &Saengsuwan, S. (2020). A one-pot microwave-assisted synthesis of IPN hydrogels based on HEMA/AM/PVA blend for enhancing Cu (II) and Pb (II) ions removal. *Journal of Environmental Chemical Engineering*, *8*(2), 103469.

[8] Fu, F., & Wang, Q. (2011).Removal of heavy metal ions from wastewaters: a review. *Journal of environmental management*, *92*(3), 407-418.

[9]Crini G, Torri G, Lichtfouse É, Kyzas GZ, Wilson LD, Morin-Crini N (2019) Cross-linked chitosan hydrogels for dye removal. In: Crini G, Lichtfouse É (eds) Chitin and chitosan—applications in food, agriculture, pharmacy, medicine and wastewater treatment, vol 35. Sustainable agriculture reviews. Springer, Basel.https ://doi. org/10.1007/978-3-030-16581 -9_10.

[10]V. Dulman, S.-M.Cucu-Man, I. Bunia and M. Dumitras: 'Batch fixed bed column studies on removal of Orange G acid dye by a weak base functionalized polymer', *Desalination and Water Treatment*, 2016, **57**, 14708–14727.

[11]J. Jordan, K. I. Jacob, R. Tannenbaum, M. A. Sharaf and I. Jasiuk:Experimental trends in polymer nanocomposites – a review', *Mater.Sci. Eng. A*, 2005, **393**, 1–11.

[12]G. Lofrano, M. Carotenuto, G. Libralato, R. F. Domingos, A. Markus,L. Dini, R. K. Gautam, D. Baldantoni, M. Rossi, S. K. Sharma, M. C.Chattopadhyaya, M. Giugni and S. Meric: 'Polymer functionalizednanocomposites for metals removal from water and wastewater: Anoverview', *Water Res.*, 2016, **92**, 22–37.

[13]Akbarnejad, S., Amooey, A. A., &Ghasemi, S. (2019). High effective adsorption of acid fuchsin dye using magnetic biodegradable polymer-based nanocomposite from aqueous solutions. *Microchemical Journal*, *149*, 103966.

[14]Sarkar, A. K., Saha, A., Panda, A. B., & Pal, S. (2015). pH Triggered superior selective adsorption and separation of both cationic and anionic dyes and photocatalytic activity on a fully exfoliated titanate layer–natural polymer based nanocomposite. *Chemical Communications*, *51*(89), 16057-16060.

[15]Gong, N., Liu, Y., & Huang, R. (2018).Simultaneous adsorption of Cu2+ and Acid fuchsin (AF) from aqueous solutions by CMC/bentonite composite. *International journal of biological macromolecules*, *115*, 580-589.

[16]Tanzifi, M., Yaraki, M. T., Karami, M., Karimi, S., Kiadehi, A. D., Karimipour, K., & Wang, S. (2018). Modelling of dye adsorption from aqueous solution on polyaniline/carboxymethyl cellulose/TiO2 nanocomposites. *Journal of colloid and interface science*, *519*, 154-173.
[17]Binaeian, E., Zadvarzi, S. B., & Yuan, D. (2020).Anionic dye uptake via composite using chitosan-polyacrylamide hydrogel as matrix containing TiO2 nanoparticles; comprehensive adsorption studies. *International journal of biological macromolecules*, *162*, 150-162.

[18]Awwad, A., Amer, M., & Al-aqarbeh, M. (2020). TiO2-kaolinite nanocomposite prepared from the Jordanian Kaolin clay: Adsorption and thermodynamics of Pb (II) and Cd (II) ions in aqueous solution. Chemistry International 6(4) (2020) 168-17.

[19]Rezakazemi, M., Sadrzadeh, M., Mohammadi, T., & Matsuura, T. (2017). Methods for the preparation of organic–inorganic nanocomposite polymer electrolyte membranes for fuel cells. In *Organic-inorganic composite polymer electrolyte membranes* (pp. 311-325). Springer, Cham.

[20]El-Sayyad, G. S., AbdElkodous, M., El-Khawaga, A. M., Elsayed, M. A., El-Batal, A. I., & Gobara, M. (2020). Merits of photocatalytic and antimicrobial applications of gamma-irradiated Co x Ni 1− x Fe2O4/SiO2/TiO2; x= 0.9 nanocomposite for pyridine removal and pathogenic bacteria/fungi disinfection: implication for wastewater treatment. *RSC Advances*, *10*(9), 5241-5259.

[21]Zhu, C. H., Hai, Z. B., Cui, C. H., Li, H. H., Chen, J. F., & Yu, S. H. (2012). In situ controlled synthesis of thermosensitive poly (N-isopropylacrylamide)/Au nanocomposite hydrogels by gamma radiation for catalytic application. *Small*, *8*(6), 930-936.

[22]Hassan, D., &Hashim, A. (2018).Preparation and Studying the Structural and Optical Properties of (Poly-Methyl Methacrylate–Lead Oxide) Nanocomposites for Bioenvironmental Applications. *Journal of Bionanoscience*, *12*(3), 346-349.

[23]Elbarbary, A. M., Ibrahim, I. A., Shafik, H. M., & Othman, S. H. (2017). Magnetic 99mTc-core-shell of polyethylene glycol/polyhydroxyethyl methacrylate based on Fe3O4 nanoparticles: Radiation synthesis, characterization and biodistribution study in tumor bearing mice. *Advanced Powder Technology*, *28*(8), 1898-1910.

[24]Elbarbary, A. M., & El-Sawy, N. M. (2017).Radiation synthesis and characterization of polyvinyl alcohol/chitosan/silver nanocomposite membranes: antimicrobial and blood compatibility studies. *Polymer Bulletin*, *74*(1), 195-212.

[25] Nagi M. El-Shafai, Rencai Ji, Mahmoud Abdelfatah, Mohamed A. Hamada, A.W. Kandeal, Ibrahim M. El-Mehasseb, Abdelhamid El-Shaer, Meng An, Mohamed S. Ramadan, Swellam W. Sharshir, Walid Ismail, (2021). Investigation of a novel (GO@ CuO. γ-Al2O3) hybrid nanocomposite for solar energy applications. *Journal of Alloys and Compounds*, *856*, 157463.

[26]Singh, K., Barai, D. P., Chawhan, S. S., Bhanvase, B. A., & Saharan, V. K. (2021). Synthesis, characterization and heat transfer study of reduced graphene oxide-Al2O3

nanocomposite based nanofluids: Investigation on thermal conductivity and rheology. *Materials Today Communications*, *26*, 101986.

[27]El-Arnaouty M.B., Abdel Ghaffar A. M. , Abdel Baky A. A., Shama S. A., (2017), J. Vinyl& Additive, 25, S1, E35-E43.

[28]Gaaz, T. S., Sulong, A. B., Akhtar, M. N., Kadhum, A. A. H., Mohamad, A. B., & Al-Amiery, A. A. (2015). Properties and applications of polyvinyl alcohol, halloysite nanotubes and their nanocomposites. *Molecules*, *20*(12), 22833-22847.

[29] Marin, E., Rojas, J., &Ciro, Y. (2014).A review of polyvinyl alcohol derivatives: Promising materials for pharmaceutical and biomedical applications. *African Journal of Pharmacy and Pharmacology*, *8*(24), 674-684.

[30]Rabiee, A. (2010). Acrylamide-based anionic polyelectrolytes and their applications: A survey. *Journal of Vinyl and Additive Technology*, *16*(2), 111-119.

[31]M. Hdidar, S. Chouikhi, A. Fattoum, M. Arous a, A. Kallel, " Multifunction applications of TiO2/poly(vinyl alcohol) nanocomposites for Laser attenuation applications " J. Alloy. Comp. 750 (2018) 375e383.

[32] J.B. Zhong, Y. Lu, W.D. Jiang, Q.M. Meng, X.Y. He, J.Z. Li, Y.Q. Chen, " Characterization and photocatalytic property of Pd/TiO2 with the oxidation of gaseous benzene" J. Hazard Mater. 168 (2009) 1632–1635.

[33]W. Zhang, Q. Deng, Q. He, J. Song, S. Zhang, H. Wang, J. Zhou, H. Zhang, A facile synthesis of core-shell/bead-like poly (vinyl alcohol)/alginate@PAM with good adsorption capacity, high adaptability and stability towards Cu(II) removal, Chem. Eng. J. 351 (2018) 462–472.

[34]E. Sonker, R. Tiwari, P. Adhikary, K. Kumar, S. Krishnamoorthi, Preparation of ultra-high-molecular-weight polyacrylamide by vertical solution polymerization technique, Polym. Eng. Sci. 59 (2019) 1175–1181.

[35]E. Sonker, R. Tiwari, P. Adhikary, K. Kumar, S. Krishnamoorthi, Preparation of ultra-high-molecular-weight polyacrylamide by vertical solution polymerization technique, Polym. Eng. Sci. 59 (2019) 1175–1181.

[36]Pourjafar, S., Rahimpour, A., &Jahanshahi, M. (2012). Synthesis and characterization of PVA/PES thin film composite nanofiltration membrane modified with TiO2 nanoparticles for better performance and surface properties. *Journal of Industrial and Engineering Chemistry*, *18*(4), 1398-1405.

[37] KheamrutaiThamaphat, PichetLimsuwan and BoonlaerNgotawornchai, Phase Characterization of TiO2 Powder by XRD and TEM, Kasetsart J. (Nat. Sci.) 42 : 357 - 361 (2008)

[38] Cao, X., Ma, J., Shi, X., &Ren, Z. (2006).Effect of TiO2 nanoparticle size on the performance of PVDF membrane. *Applied Surface Science*, *253*(4), 2003-2010.

[39]Pakdel, P. M., &Peighambardoust, S. J. (2018). Review on recent progress in chitosan-based hydrogels for wastewater treatment application. *Carbohydrate polymers*, *201*, 264-279.

[40]I. Langmuir, "THE ADSORPTION OF GASES ON PLANE SURFACES OF GLASS, MICA AND PLATINUM" J. Am. Chem. Soc., 1918, 40, 1361–1403.

[41] H. Freundlich, "Of the adsorption of gases. Section II. Kinetics and energetics of gas adsorption.Introductory paper to section II" Trans. Faraday Soc., 1932, 28, 195–201.

[42]Tanzifi, M., Yaraki, M. T., Karami, M., Karimi, S., Kiadehi, A. D., Karimipour, K., & Wang, S. (2018). Modelling of dye adsorption from aqueous solution on polyaniline/carboxymethyl cellulose/TiO2 nanocomposites. *Journal of colloid and interface science*, *519*, 154-173.

[43]Abdulhameed, A. S., Mohammad, A. T., &Jawad, A. H. (2019). Application of response surface methodology for enhanced synthesis of chitosan tripolyphosphate/TiO2 nanocomposite and adsorption of reactive orange 16 dye. *Journal of Cleaner Production*, *232*, 43-56.

[44] Elbarbary, A. M., & Ghobashy, M. M. (2017).Phosphorylation of chitosan/HEMA interpenetrating polymer network prepared by γ-radiation for metal ions removal from aqueous solutions. *Carbohydrate polymers*, *162*, 16-27.

[45] Gong, N., Liu, Y., & Huang, R. (2018).Simultaneous adsorption of Cu2+ and Acid fuchsin (AF) from aqueous solutions by CMC/bentonite composite. *International journal of biological macromolecules*, *115*, 580-589.

[46]Jung, K. W., Lee, S. Y., Choi, J. W., & Lee, Y. J. (2019). A facile one-pot hydrothermal synthesis of hydroxyapatite/biocharnanocomposites: adsorption behavior and mechanisms for the removal of copper (II) from aqueous media. *Chemical Engineering Journal*, *369*, 529-541.

[47]Lagergren S, Svenska BK (1898) On the theory of socalled adsorption of dissolved substances, *R. Swed.Acad. Sci. Doc. Band*, 24 1–39.

[48] Ho YS, (2004) Citation Review of Lagergren Kinetic Rate Equation on Adsorption Reactions, *Scientometrics*, 59, 171-177.

[49] A. Masoumi, K. Hemmati and M. Ghaemy, "Structural modification of acrylonitrile–butadiene–styrene waste as an efficient nanoadsorbent for removal of metal ions from water: isotherm, kinetic and thermodynamic study", RSC Adv., 2015, 5, 1735–1744.

[50]G. Bayramoglu, B. Altintas and M. Y. Arica, "Adsorption kinetics and thermodynamic parameters of cationic dyes from aqueous solutions by using a new strong cation-exchange resin", Chem. Eng. J., 2009, 152, 339–346.

[51]Gobi, K., M. Mashitah, and V. Vadivelu, Adsorptive removal of methylene blue using novel adsorbent from palm oil mill effluent waste activated sludge: equilibrium, thermodynamics and kinetic studies. Chemical engineering journal, 2011. 171(3): p. 1246-1252.

Figures

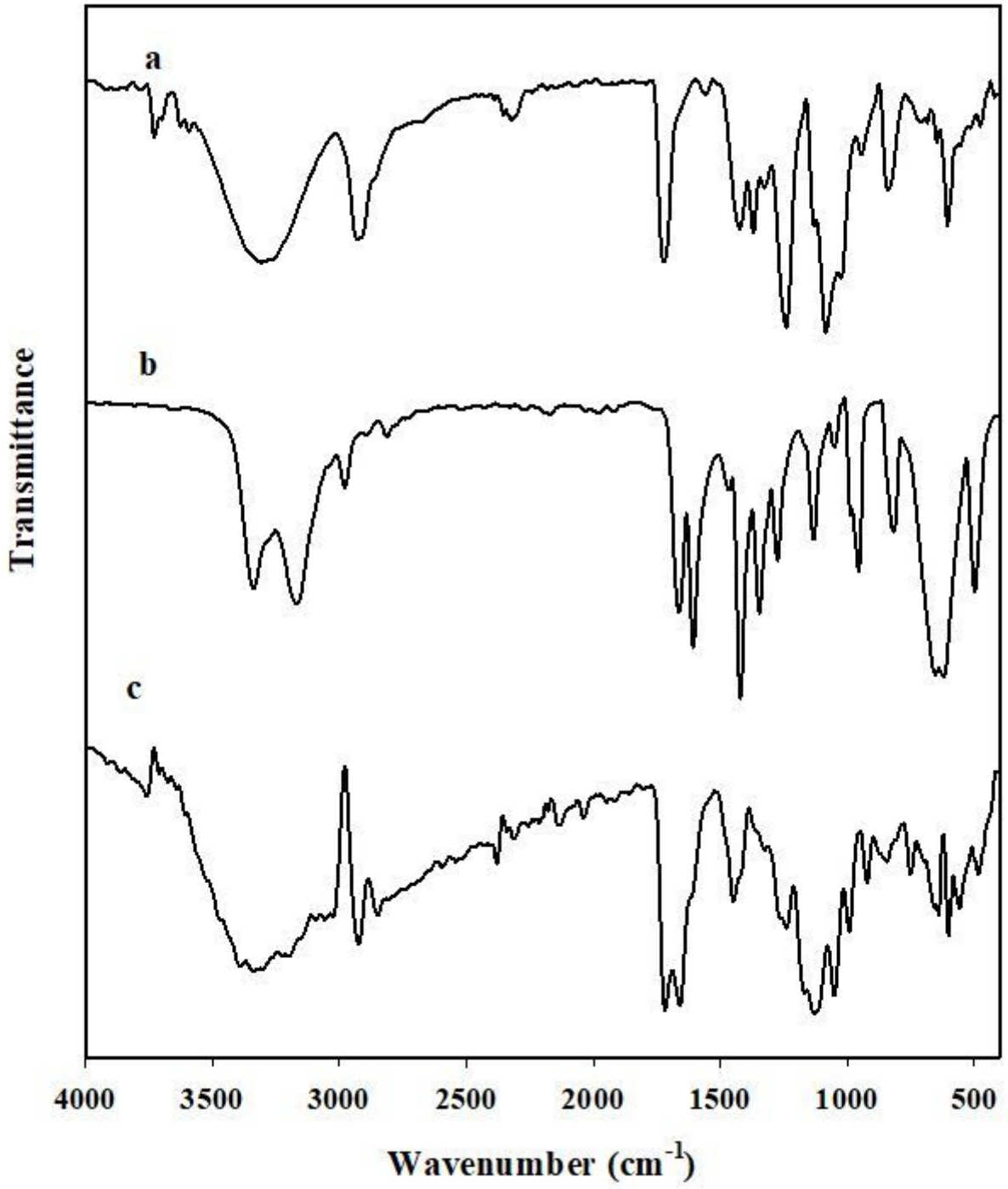

Figure 1

FTIR spectra of (a) PVA, (b) AAm and (c) PVA-co-AAm/TiO2/SiO2 nanocomposite.

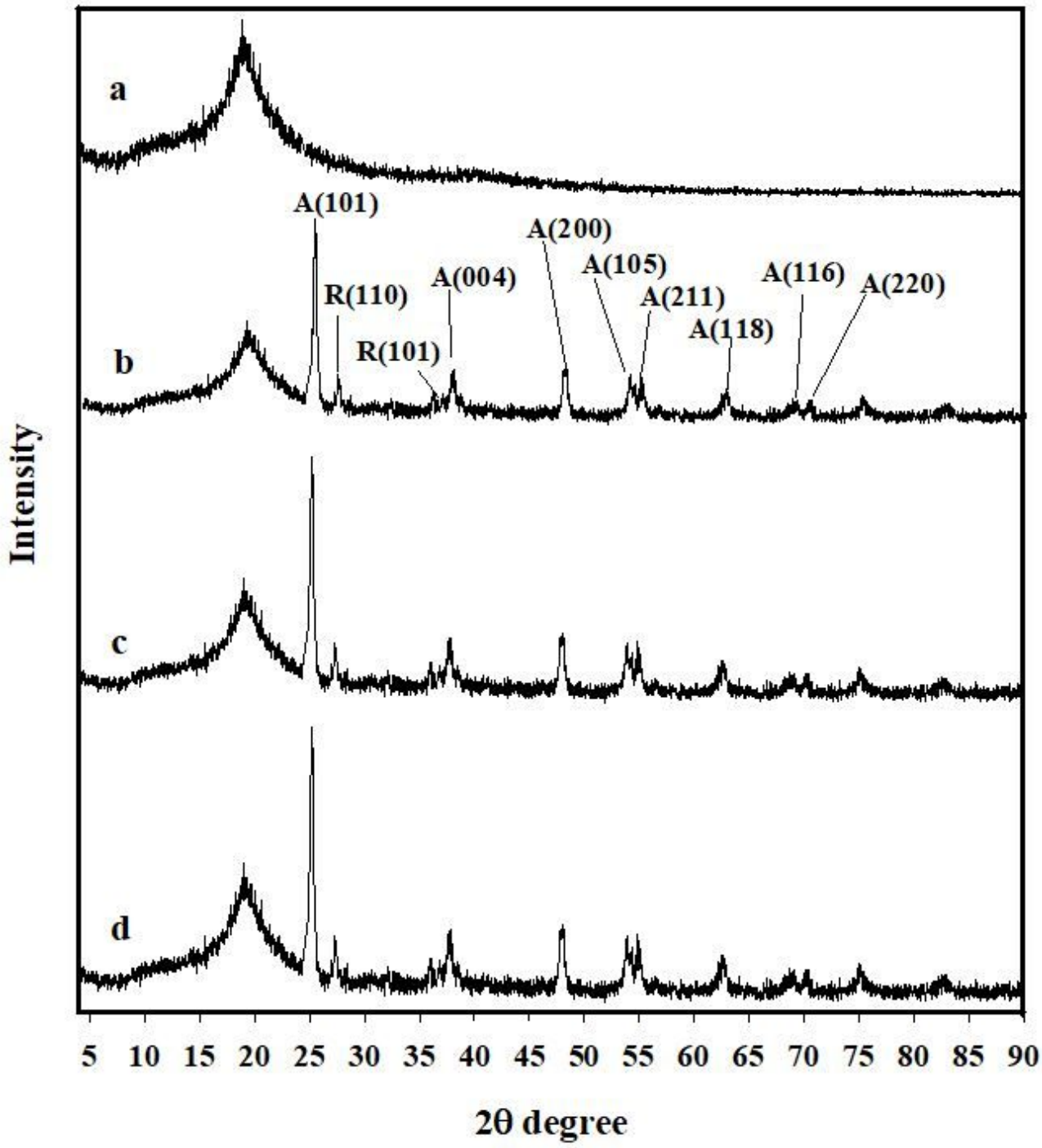

Figure 2

XRD curves of (a) PVA-co-AAm, (b) PVA-co-AAm/TiO2/SiO2-10 (c) PVA-co-AAm/TiO2/SiO2-30 and (d) PVA-co-AAm/TiO2/SiO2-50 nanocomposites.

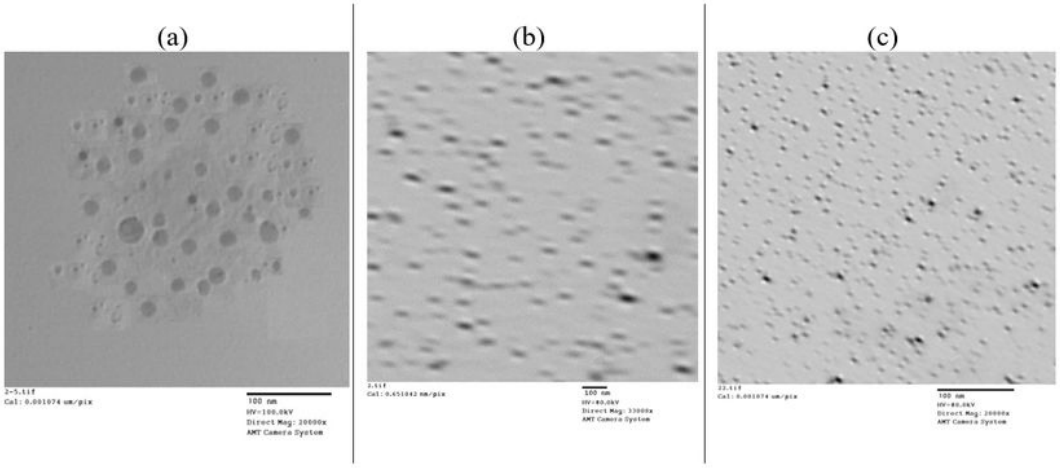

(d)

Mean Diameter	= 93.5 nm	Variance (P.I.)	= 0.296
Stnd. Deviation	= 44.7 nm (16.4%)	Chi Squared	= 40.6
Norm. Stnd. Dev. (Coeff. of Var'n)	= 0.544	Baseline Adj.	= 0.000 %
		Z-Avg. Diff. Coeff.	= 4.99E-009 cm2/s

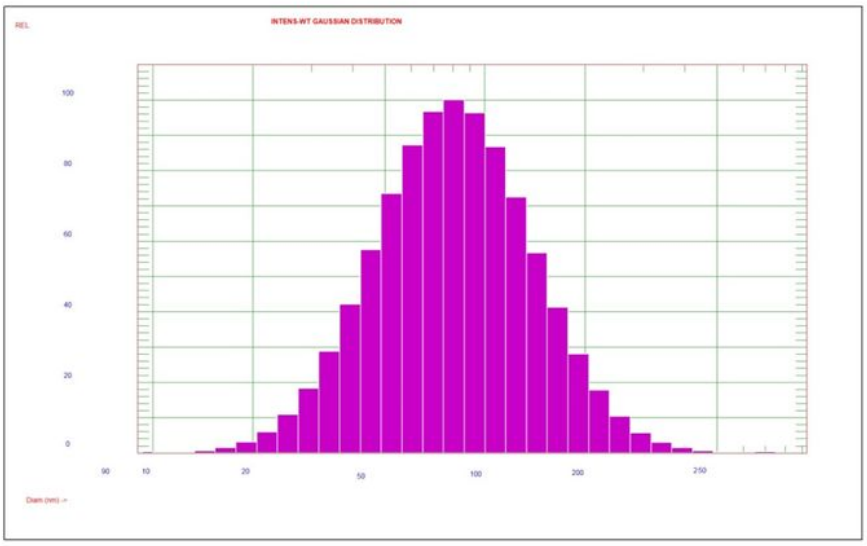

Figure 3

TEM images of (a) PVA-co-AAm/TiO2/SiO2 -10, (b) PVA-co-AAm/TiO2/SiO2-30 and (c) PVA-co-AAm/TiO2/SiO2-50. (d) DLS of PVA-co-AAm/TiO2/SiO2-30 nanocomposite.

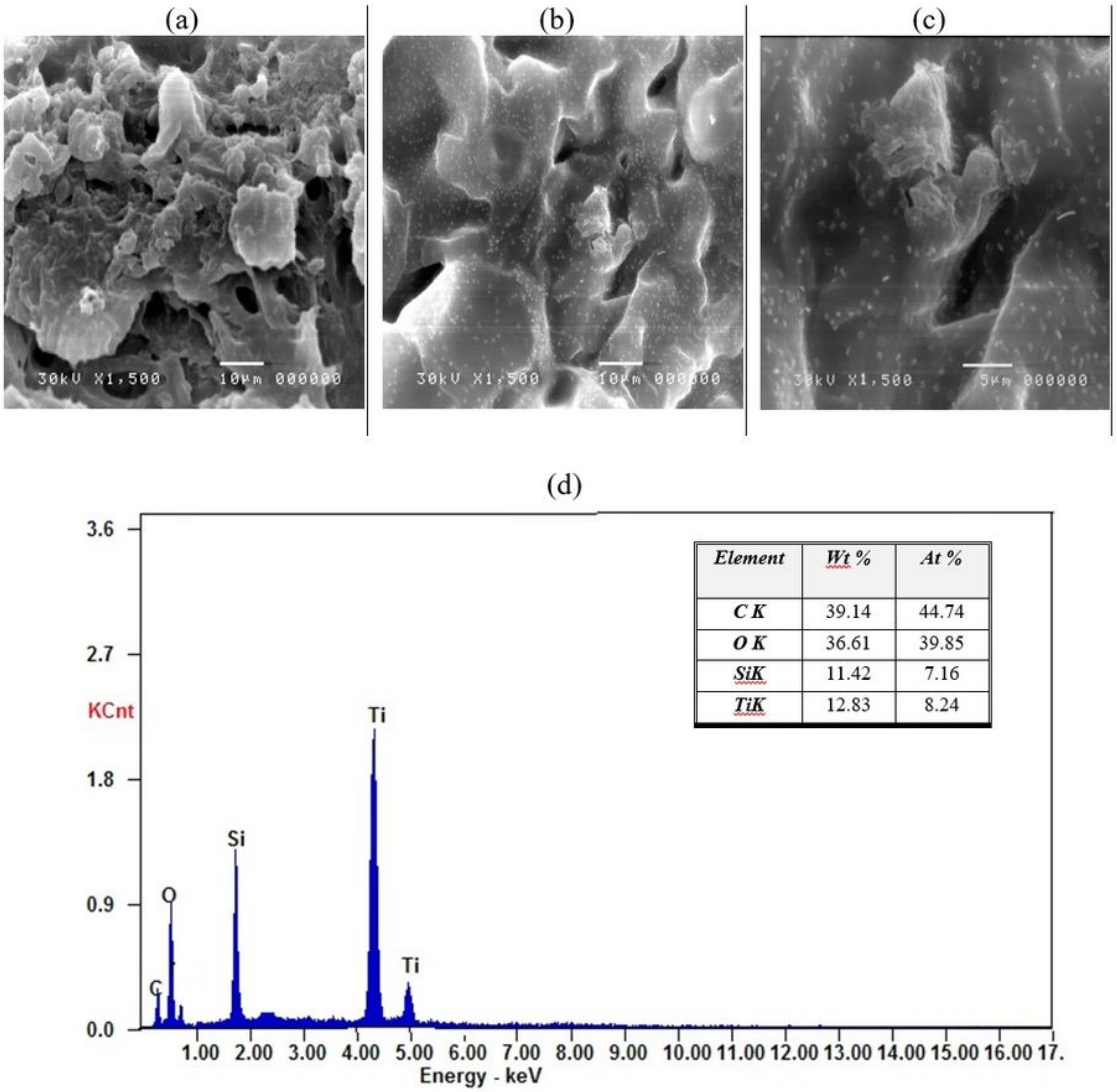

Figure 4

SEM micrographs of(a) PVA-co-AAm/TiO2/SiO2-10 (b) PVA-co-AAm/TiO2/SiO2-30 and (c) PVA-co-AAm/TiO2/SiO2-50.(d) SEM/EDX spectrum of PVA-co-AAm/TiO2/SiO2-30 nanocomposite.

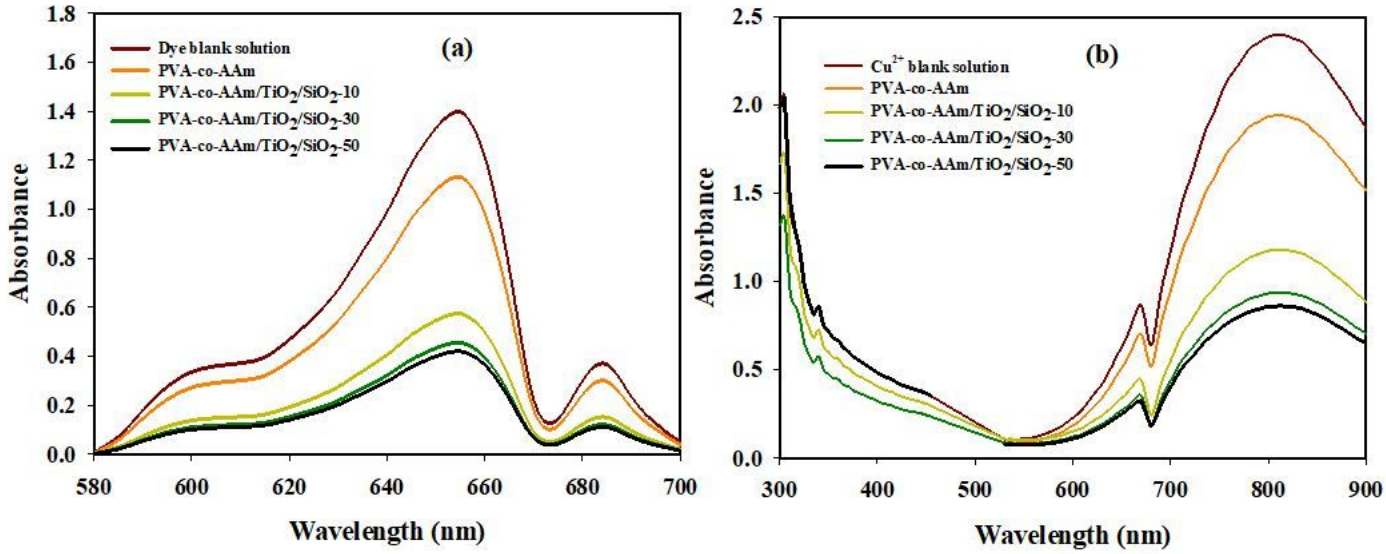

Figure 5

UV absorption spectra of (a) basic blue 3 dye and (b) Cu (II) ions by the effect of the prepared PVA-co-AAm and PVA-co-AAm/TiO2/SiO2 nanocomposites.

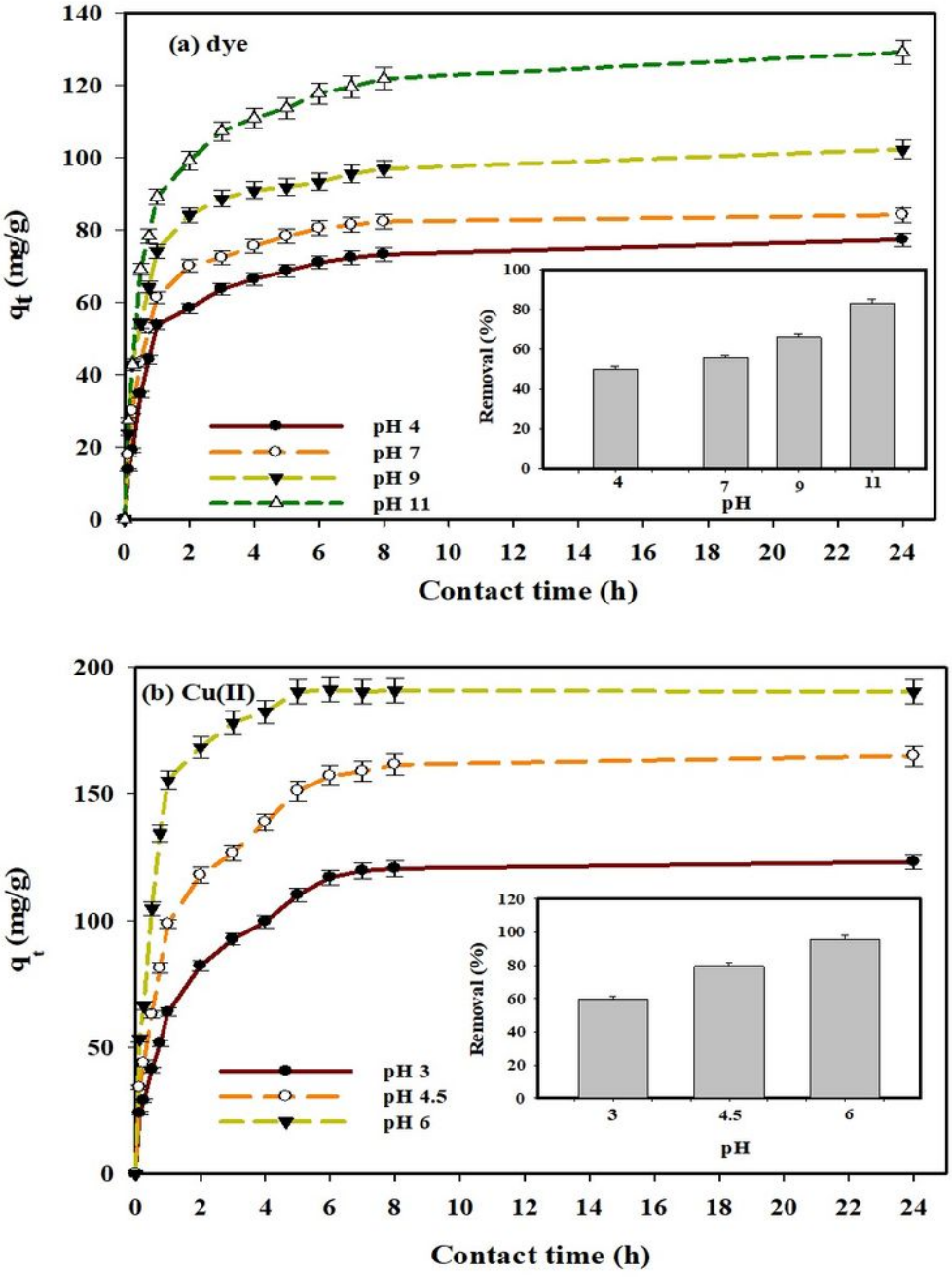

Figure 6

Effect of pH and contact time (h) on the amount adsorbed (qt) (mg/g) and removal (%) of (a) basic blue 3 dye and (b) Cu (II) ions onto PVA-co-AAm/TiO2/SiO2 nanocomposite (initial concentration 150 mg/L for the dye and 200 mg/L for Cu (II) ions; adsorbent dosage 0.3 g; temperature 298 K; agitation speed 100 rpm).

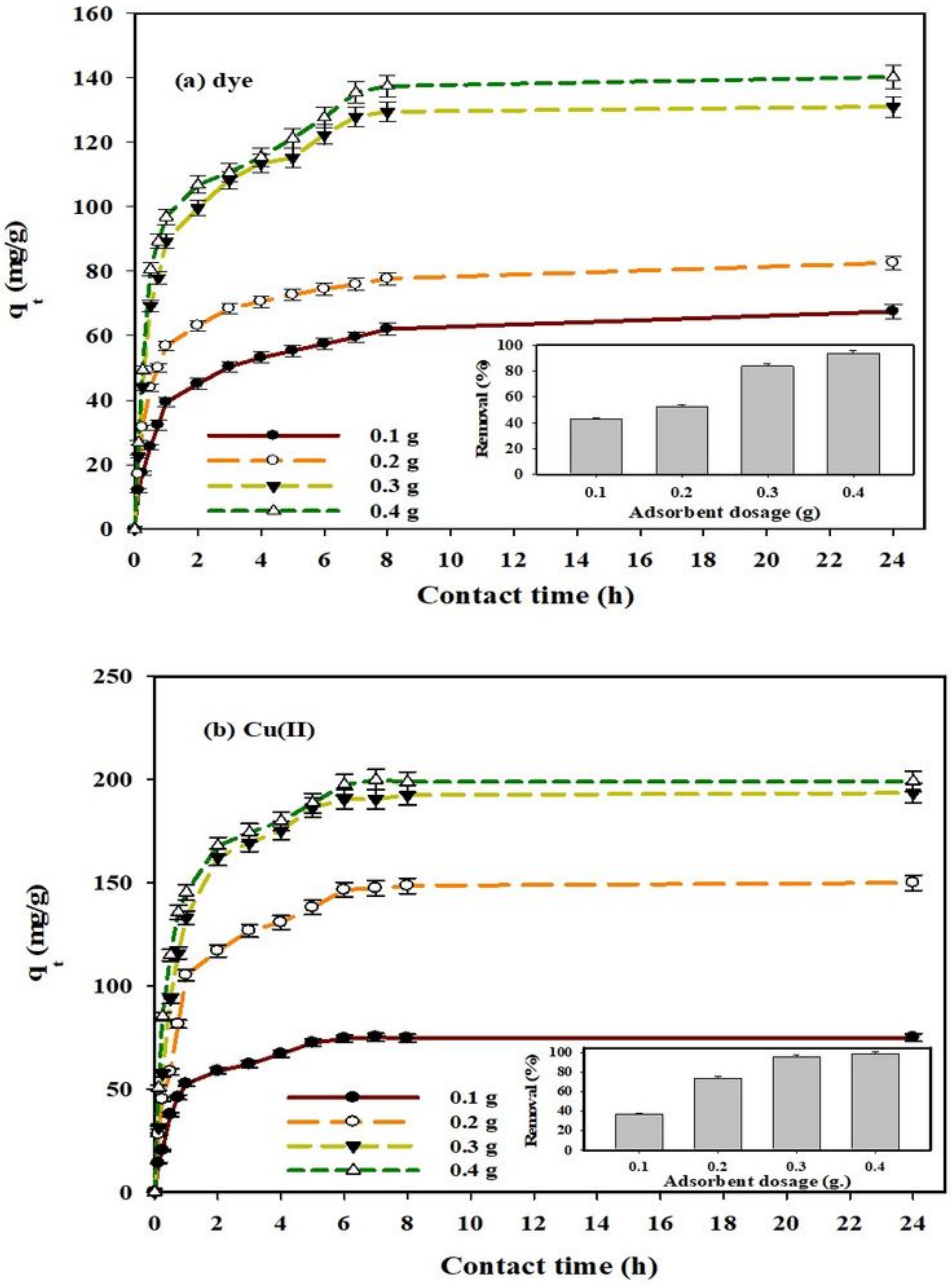

Figure 7

Effect of adsorbent dosages and contact time (h) on the amount adsorbed (mg/g) of the (a) basic blue 3 dye and (b) Cu (II) ions onto the PVA-co-AAm/TiO2/SiO2-30 nanocomposite (pH 11 for the dye and pH 6 for Cu (II); initial concentration 150 mg/L for the dye and 200 mg/L for Cu (II) ions; temperature 298 K; agitation speed 100 rpm).

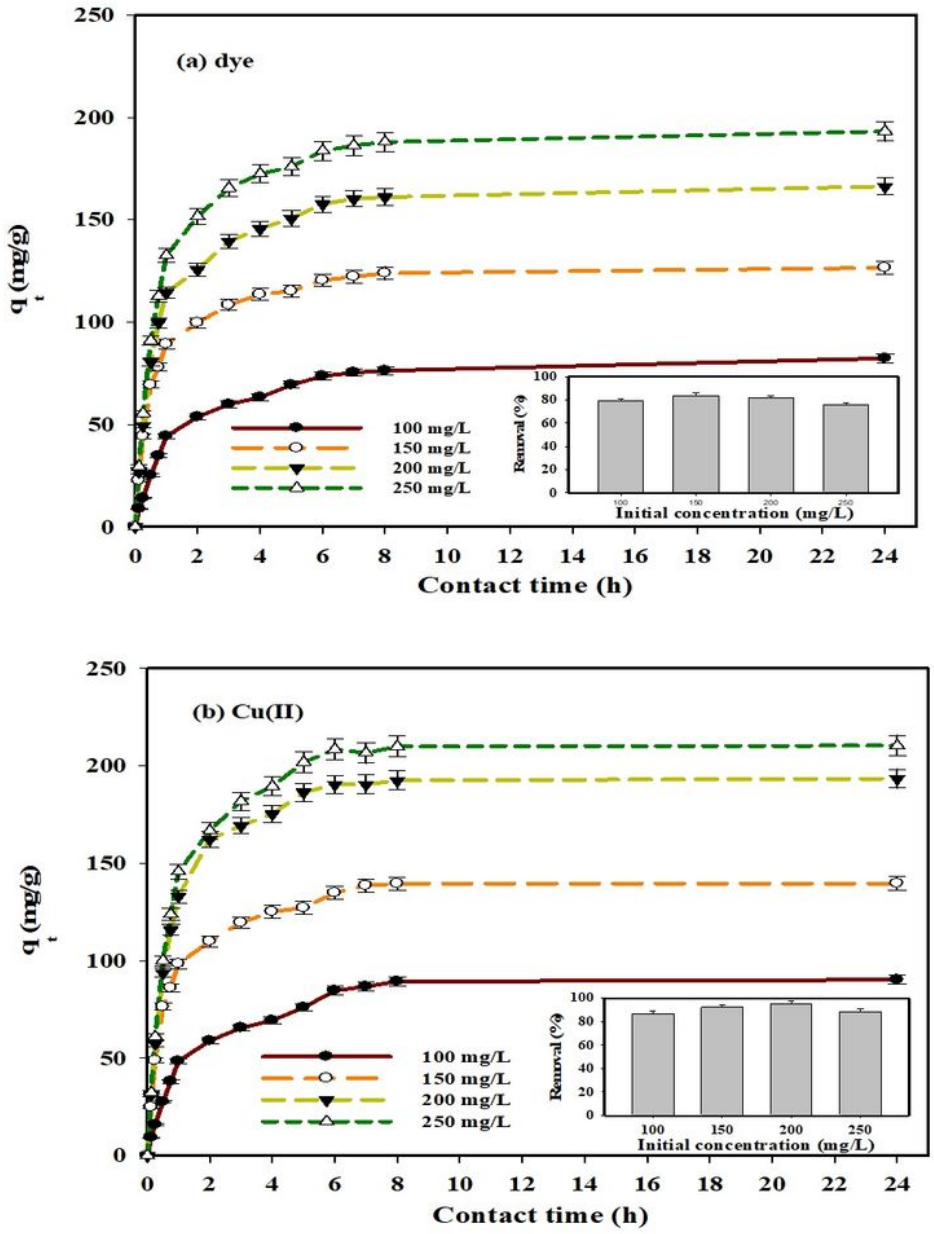

Figure 8

Impact of initial concentration (mg/l) with contact time (h) onto the amount adsorbed (mg/g) and removal (%) of the (a) basic blue 3 dye and (b) Cu (II) ions onto the PVA-co-AAm/TiO2/SiO2-30 nanocomposite (pH 11 for the dye and pH 6 for Cu (II), 0.3 g adsorbent dosage. temperature 298 K; agitation speed 100 rpm).

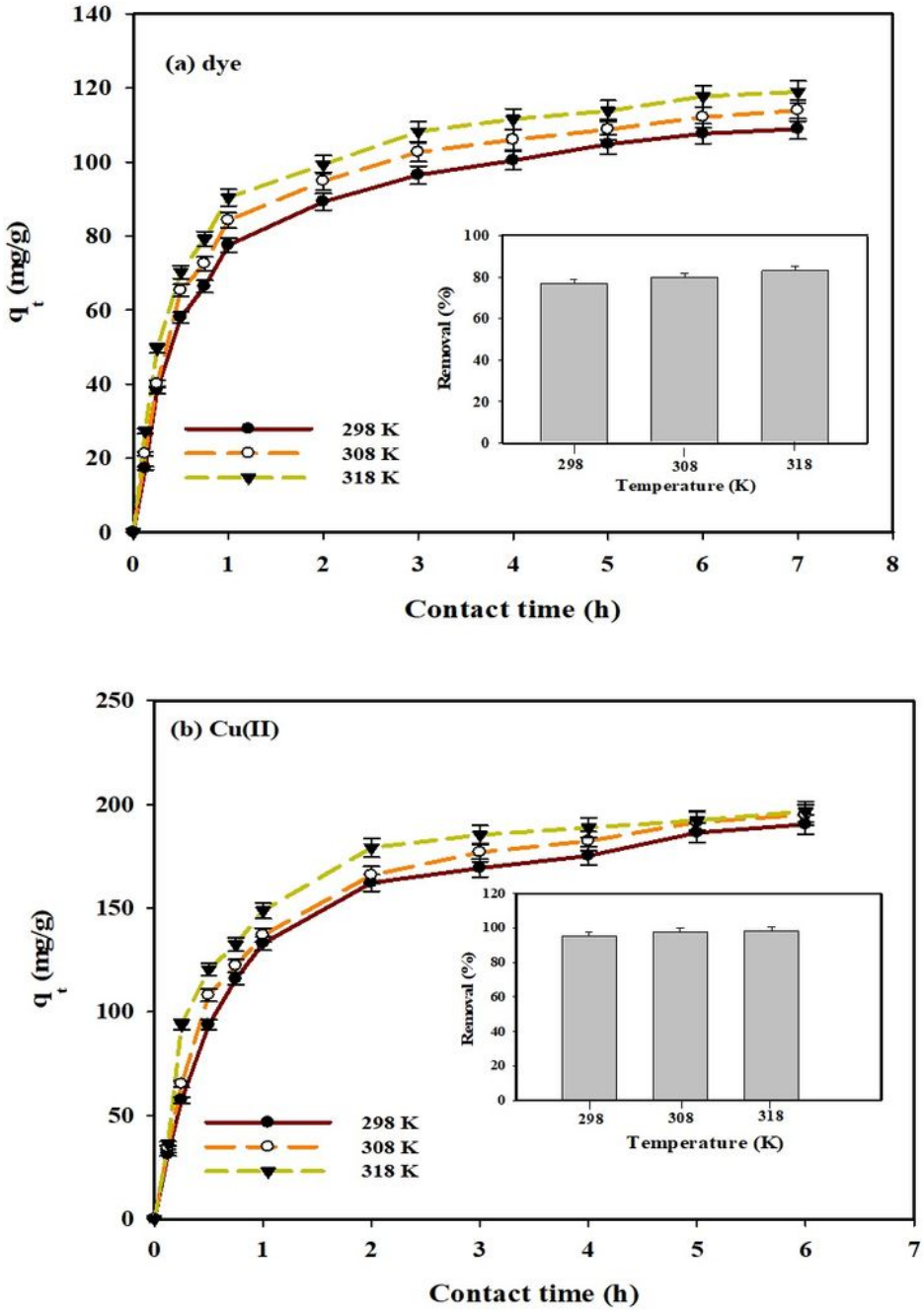

Figure 9

Impact of temperature (K) with contact time (h) onto the amount adsorbed (mg/g) and removal (%) of the (a) basic blue 3 dye and (b) Cu (II) ions onto PVA-co-AAm/TiO2/SiO2-30 nanocomposite (pH11 for the dye and pH 6 for Cu (II) ions; contact time 7h for the dye and 6 h for Cu (II); 0.3 g adsorbent dosage; initial concentration 150 mg/L for the dye and 200 mg/L for Cu (II) ions; agitation speed 100 rpm).

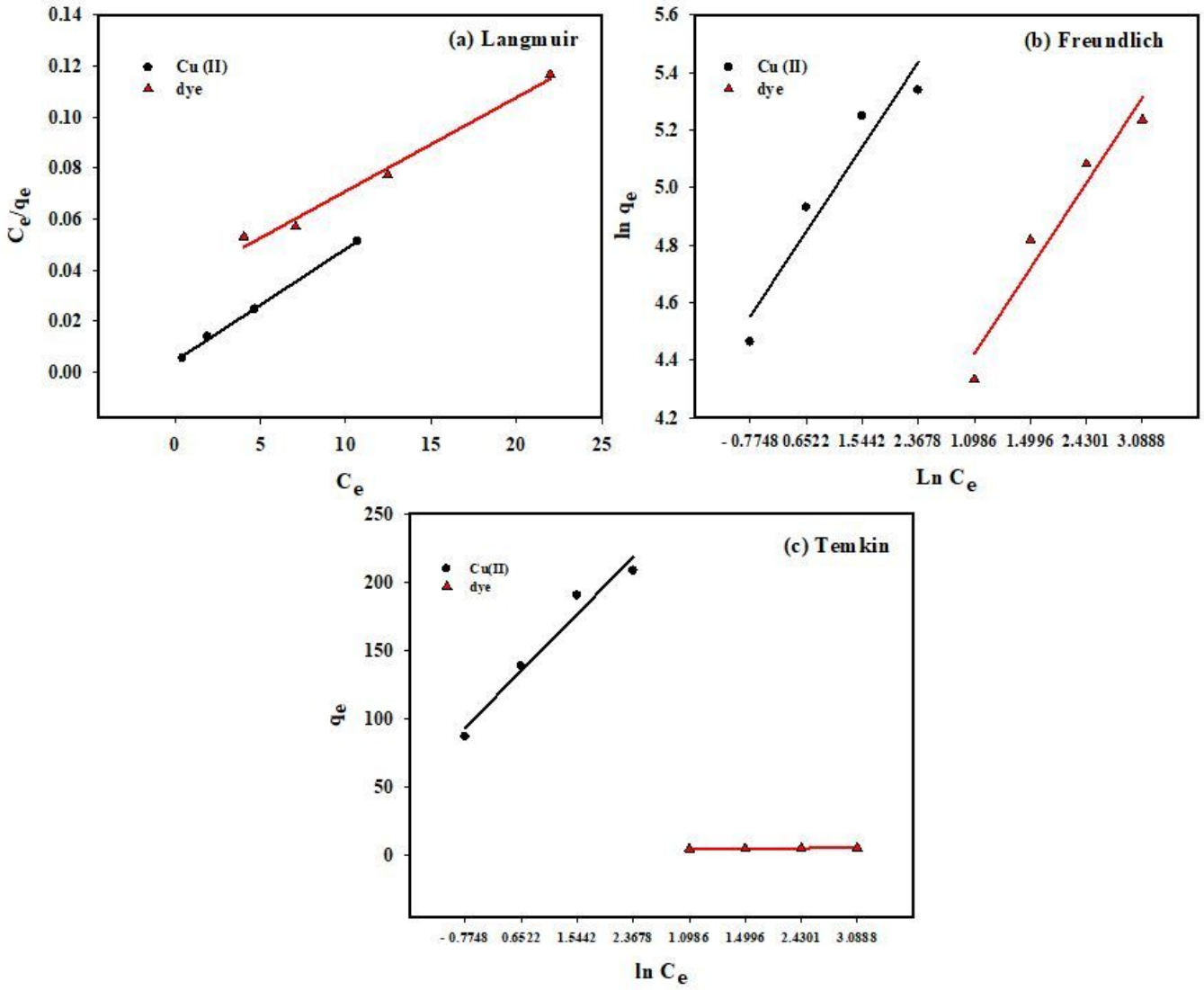

Figure 10

(a) Langmuir, (b) Freundlich and (c) Temkin isotherm for adsorption of basic blue 3 dye and Cu (II) ions onto PVA-co-AAm/TiO2/SiO2-30 nanocomposite.

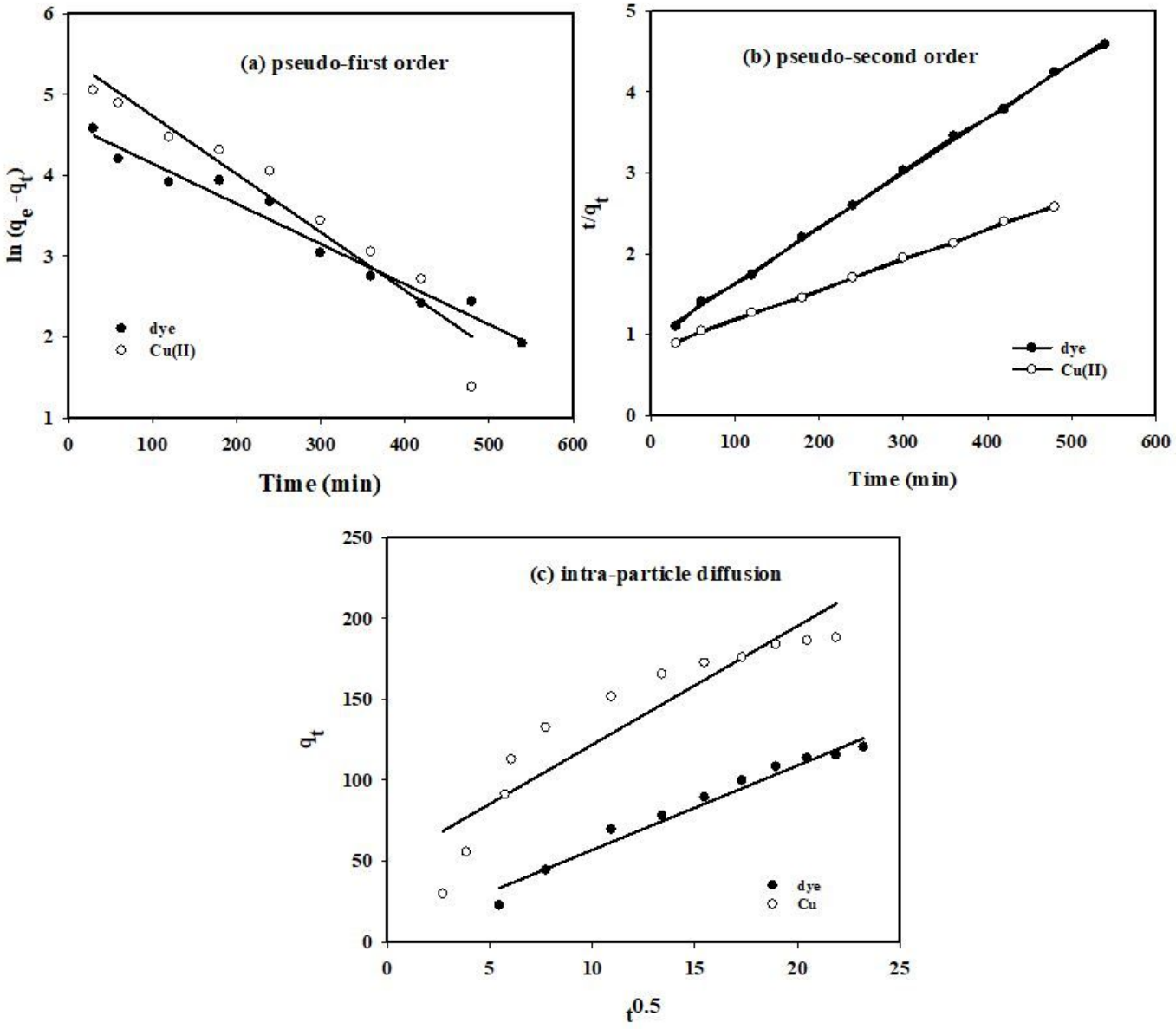

Figure 11

plots of (a) pseudo first order, (b) pseudo second order and (c) intra-particle diffusion kinetic models applied for adsorption of basic blue 3 dye and Cu(II) ions onto PVA-co-AAm/TiO2/SiO2-30 nanocomposite.

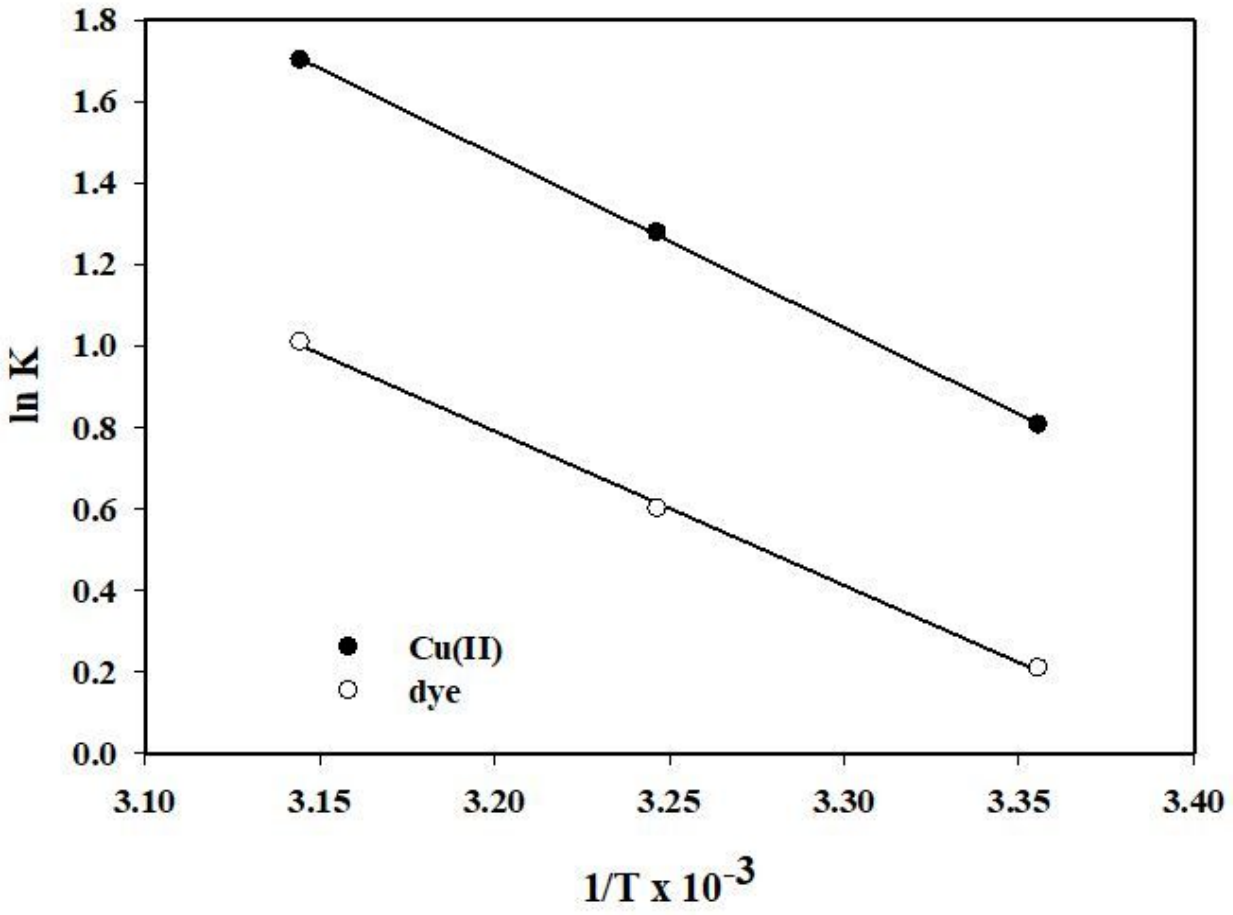

Figure 12

Van't Hoff plots of the Cu (II) ions and basic blue 3 dye adsorption at different temperatures (50 ml of initial concentration 150 mg/l for the dye and 200 mg/l for Cu(II) ions; 0.3 g adsorbent dosage, pH 6 for Cu (II) and pH 11 for the dye; contact time 6 h for Cu (II) and 7 h for the dye).

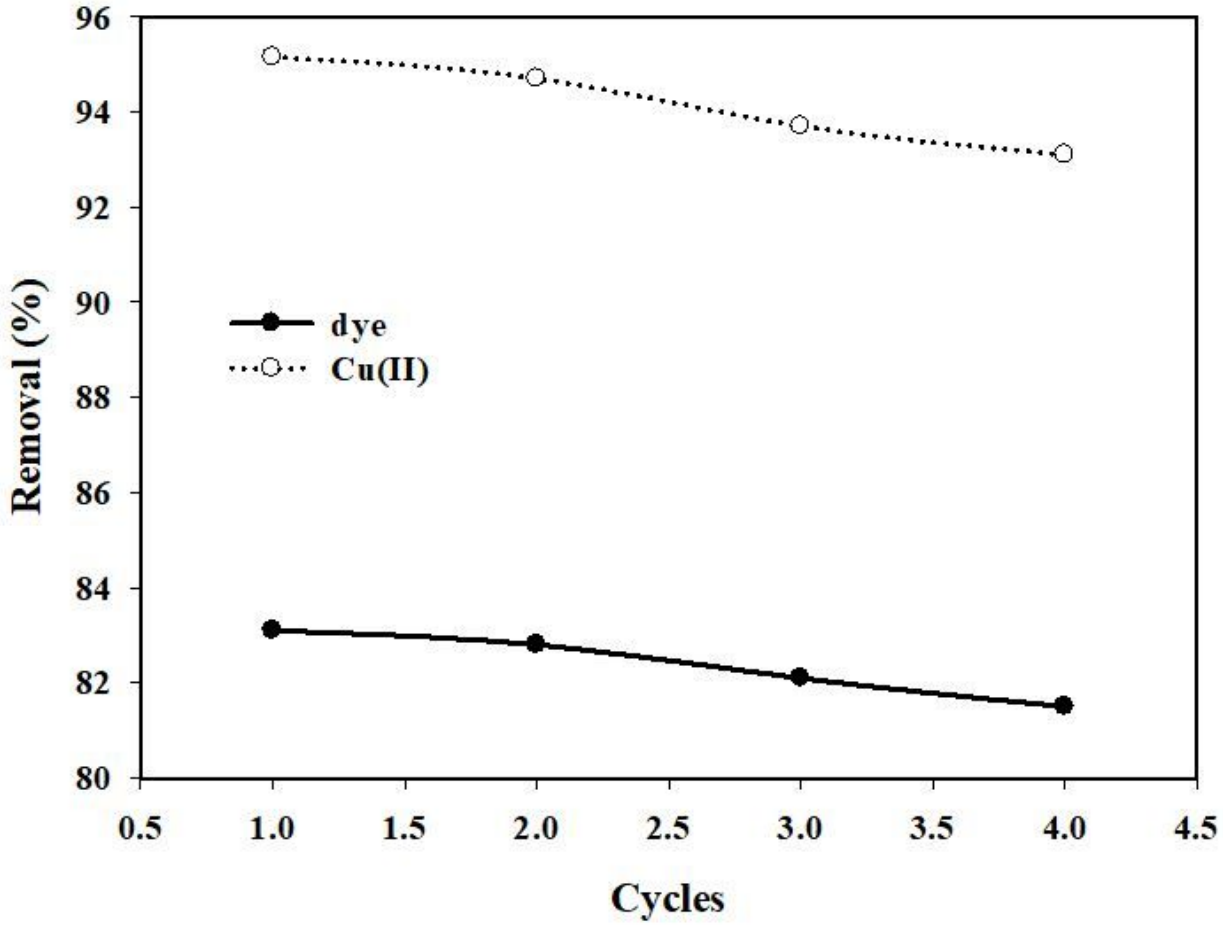

Figure 13

effect of cycle times on removal (%) of basic blue 3 dye and Cu(II) onto PVA-co-AAm/TiO2/SiO2-30 nanocomposite